2010

Production Of Activated Carbon From Fermentation And Pyrolysis Residues

Dan Cheng
North Carolina Agricultural and Technical State University

Recommended Citation
Cheng, Dan, "Production Of Activated Carbon From Fermentation And Pyrolysis Residues" (2010). *Theses*. 12.
https://digital.library.ncat.edu/theses/12

PRODUCTION OF ACTIVATED CARBON FROM FERMENTATION AND PYROLYSIS RESIDUES

by

Dan Cheng

A thesis submitted to the graduate faculty
in partial fulfillment of the requirements for the degree of
MASTER OF SCIENCE

Department: Civil & Environmental Engineering
Major: Civil & Environmental Engineering
Major Professor: Dr. Lijun Wang

North Carolina A&T State University
Greensboro, North Carolina
2010

School of Graduate Studies
North Carolina Agricultural and Technical State University

This is to certify that the Master's Thesis of

Dan Cheng

has met the thesis requirements of
North Carolina Agricultural and Technical State University

Greensboro, North Carolina
2010

Approved by:

Dr. Lijun Wang Major Professor	Dr. Abolghasem Shahbazi Committee Member
Dr. Shamsuddin Ilias Committee Member	Dr. Sameer A. Hamoush Department Chairperson

Dr. Alan Letton
Interim Associate Vice Chancellor for Research and Graduate Dean

BIOGRAPHICAL SKETCH

Dan Cheng was born in 1986 and grew up in the city of Taiyuan, China. He earned his BS from the Department of Agricultural Engineering at China Agricultural University in 2008. During the period of college education, he achieved excellence academic performance while he also involved many campus activities. Dan was a positive volunteer in serving in many non-profit social activities. After graduation, he was awarded a research assistantship to pursue his MS degree in Department of Biosystems and Agricultural Engineering at Oklahoma State University. In 2009, Dan transferred from Oklahoma State University to North Carolina Agricultural and Technical State University, continuing his master education in Civil and Environmental Engineering. He worked on a project titled “activated carbon production from fermentation and pyrolysis residues” toward his master thesis. Dan has been awarded for his excellent academic performance. His GPA for the master degree program is 3.84.

Dan is a member of American Society of Agricultural and Biological Engineers. He has participated in 2010 ASABE international conference and made an oral presentation on activated carbon production.

After finishing his MS studies, Dan is going to serve as an engineer in environmental engineering related industries.

ACKNOWLEDGEMENT

I would deeply thank and appreciate my academic advisor, Dr. Lijun Wang, for his academic and research assistance and financial support. Dr. Wang, a knowledgeable professor, not only taught me a lot in academics and research, but also instructed me on my path in the future. I would like to thank Dr. Abolghasem Shahbazi, the Director of Biological Engineering Program, for his dedication and efforts in helping me with this research.

I would like to express my appreciation to Dr. Shamsuddin Ilias and his graduate student Mr. Md. Saiful Islam for their help in characterizing activated carbon, Dr. Mohamed Ahmedna and his graduate student Djaarfar Rehrah for their help in the preparation of activated carbon, Dr. G.B. Reddy and his lab technician for their help in the elemental analysis.

I also want to take this opportunity to thank all fellow researchers and staff in the Biological Engineering Program for their help through this research.

Finally, I would like to thank my mother and my father for believing in me, encouraging me, and supporting me.

TABLE OF CONTENTS

LIST OF FIGURES

FIGURES **PAGE**

LIST OF TABLES

TABLES **PAGE**

ABSTRACT

Cheng, Dan. PRODUCTION OF ACTIVATED CARBON FROM FERMENTATION AND PYROLYSIS RESIDUES. (**Major Advisor: Lijun Wang**), North Carolina Agricultural and Technical State University.

The objective of this study is to produce activated carbon from fermentation and pyrolysis residues. It was found that both fermentation and pyrolysis residues are highly appropriate as precursors for activated carbon production because of their high carbon content and low ash content. The effects of activation temperature, activation time and phosphoric acid concentration on the yield and quality of activated carbon were investigated. Increased activation temperature, activation time and acid concentration have similar effect of decreasing the yield of activated carbon. Increased activation temperature and activation time decreases the BET surface area and pore volume of activated carbon while impregnating acids at too low and too high concentrations decreases the BET surface area and pore volume. The maximum BET surface area and pore volume were found to be 513 m^2/g and 0.302 cc/g, respectively, for the activated carbon produced from the fermentation residues impregnated with 20% phosphoric acid and subsequently activated at 450°C for 1 h. Under these conditions, the yield of activated carbon was 51%. Activated carbon produced from pyrolysis residues had a surface area above 800 m^2/g, which was higher than that produced from fermentation residues.

Research on the Fe catalyst supported on activated carbon showed activated carbon produced from pyrolysis residues had better adsorption capability for Fe than that of fermentation residues. Catalysts developed on activated carbons from fermentation and pyrolysis residues are stable at 200°C for 2 h.

Economic analysis shows that the cost of activated carbon produced from fermentation residues is lower than that of activated carbon from pyrolysis residues. Activated carbon can be more economically produced as the size of the facility is increased.

CHAPTER 1

INTRODUCTION

Activated carbon, which has a very large surface area and micro-pore volume, is considered as one of the most important adsorbents. In recent years, as the rapid development of chemistry industry, activated carbon is very popular in catalyst development, in which it is used as a catalyst support. As more and more attention and concern are casted into environmental areas, activated carbons have found more and more applications in resolving environmental issues such as waste water treatment. On the whole, the demand for activated carbons has significantly increased during the past several decades.

Any raw material that is rich in carbon and low in ash can be used as a precursor to produce activated carbon. The first generation of activated carbon was produced from coal and wood. However, coal is a non-renewable source and the use of wood to produce activation carbon will compete with furniture manufacture. Various research has been done on the production of activated carbon from agricultural residues and by-products such as sugar bagasse and rice husk. Agricultural residues and by-products have a great potential in activated carbon production in terms of both economic viability and the adsorptive capacity of the activated carbons.

As a result of the soaring consumption of energy in the US and the fast depletion of the fossil fuels, bio-energy has been gradually becoming a potential and competitive alternative to fossil energy resource. In the United States, bio-ethanol has become one of the largest bioenergy sectors. Most of bio-ethanol is currently produced by the fermentation of corn starch in the United States. However, research has found that starch-based bio-ethanol cannot actually reduce the net green house gas emission effectively and it also competes with the food supply. More and more research has been conducted to produce bio-ethanol from lignocellulosic biomass such as switch grass, wheat straw, corn stover and cattail.

Lignocellulosic biomass is a polymer of cellulose, hemicellulose and lignin. Sugars hydrolyzed from cellulose and hemicellulose can be fermented to ethanol. In the process of lignocellulosic ethanol, lignin is left as fermentation residues. In industry, fermentation residues have very low economic value and are usually discarded as wastes or burned in a boiler for the supply of heat. Fermentation residues have a great potential to be converted to activated carbons as the lignin, which is a dominant component in fermentation residues, has a high carbon content and the fermentation residues have a very low ash content because the pretreatment and fermentation processes wash away some ash in the raw biomass.

Pyrolysis provides a method to produce bio-oil from highly distributed agricultural residues with low bulk densities and wide variations in properties. Dry agricultural residues can be thermally pyrolyzed into bio-oil in the absence of oxygen or air at a temperature of 500^{o}C or above. The rate and extent of decomposition of each component in agricultural residues depends on the pyrolytical conditions including temperature, biomass heating rate and pressure. During pyrolysis, most of biomass is converted into bio-oil. Some portion of the biomass is converted to bio-char and gas. Bio-char is usually used to improve the quality of soil by increasing the capacity of soil to retain moisture and control the release of fertilizers. Bio-char may also have a great potential to be converted to activated carbon because it has a high carbon content and rudimentary porosity acquired during pyrolysis.

Activated carbon can be produced either by physical or chemical activation. Physical activation is a two-stage process that includes carbonization of raw materials into bio-chars in an inert gas atmosphere and activation of bio-chars in an oxidizing gas agent such as steam or CO_2. As physical activation requires much higher temperature than chemical activation, it is less popular in activated carbon production. Carbonization and activation during chemical activation occur simultaneously after raw materials are impregnated with various chemicals. However, chemical activation requires a large amount of chemicals to prepare high quality activated carbon, and a lot of water and energy to clean the activation carbon.

The goal of this study is to upgrade different bio-refinery residues including fermentation residues and pyrolysis residues into a value-added product of activated carbon.

Specific objectives are:

Objective 1: to investigate if lignocellulosic fermentation residues and pyrolysis residues are appropriate precursors for the production of activated carbon.

Objective 2: to develop and optimize an environmentally-friendly process for the production of activated carbon from the bio-refinery residues.

Objective 3: to compare the quality of activated carbons produced from fermentation, pyrolysis and agricultural residues.

Objective 4: to develop catalysts supported on the activated carbons produced from fermentation and pyrolysis residues.

Objective 5: to investigate if activated carbons produced from fermentation and pyrolysis residues are economically viable.

CHAPTER 2

LITERATURE REVIEW

Activated carbon is a form of carbon that possesses a large surface area and micro-pore volume. Activated carbon is considered to be one of the most widely-used and efficient adsorbents in many different industries. It has already found many applications in environmental areas such as water remediation, removal of heavy metals and phenols. Activated carbon is widely used for gas storage and purification. Activated carbon is also used as a catalyst support.

2.1 Materials for Activated Carbon Production

2.1.1 Coal

Activated carbons can be produced from various carbonaceous materials which are rich in carbon and low in ash. Typical materials that are used as precursors to produce activated carbons are coals [1-3] and woods [4-5].

A three-step process was developed to produce activated carbons from Illinois basin bituminous coal: oxidation, devolatilization and activation [1]. It was found the oxidation of the coal in air at 150°C for 40 h was an effective pretreatment method to significantly develop the surface area of the coal derived activated carbon because without the oxidation pretreatment, the thermal plastic property of bituminous coal might generate coal-cake that prevents the development of micro-pore during devolatilization and activation. The optimum oxidation temperature and devolatilization and activation temperature were found to be 225°C and 860°C, respectively, in terms of the quality of activated carbon and the processing time. The activated carbons produced by the three-step process were found to have much higher capacity to absorb toluene than commercial activated carbons. The economics of the three-step process was also very favorable in terms of the cost per unit surface area of the activated carbon produced.

Hsu and Teng studied the influence of different impregnation reagents including KOH while H_3PO_4 and $ZnCl_2$ on the quality of activated carbon produced from bituminous coal [2]. They found that the impregnation of bituminous coal with KOH achieved the highest surface area of 3300 m^2/g. The reagents of H_3PO_4 and $ZnCl_2$ could not be used to produce activated carbons with a high surface area because they could not effectively prevent the formation of tar during carbonization. However, the yield of activated carbon produced with KOH was lower than that with $ZnCl_2$ and H_3PO_4, because the activation of KOH impregnated coal required higher temperature, which decreased the yield of final product of activated carbons. They also found that the increase in the particle size of the bituminous coal reduced both the yield and the porosity of the activated carbons.

There are several challenges to produce activated carbon from coal. Minerals in coals will be left in the activated carbon without any contribution to the development of surface area of the activated carbon. Furthermore, some coals will be melt to form a fluid during thermal treatment and become a char coke, which will destroy the porosity development [1, 3]. The formation of char coke can be minimized or eliminated by the oxidation pretreatment of coal [1].

2.1.2 Woody biomass

In recent years, forestry wastes have become more and more popular as raw materials to produce activated carbons due to their low supply cost [4]. Research has showed that the activated carbon produced from chestnut wood impregnated with H_3PO_4 had a BET surface area from 21-783 m^2/g [5]. Although the surface area of the chestnut wood derived activated carbon was not very high, the yield of the activated carbon in the range from 37.2 to 42.3% is very high due to the low volatile matter content of chestnut wood. It was also found that the micro-pore volume and BET surface area decreased when the temperature was increased up to 600°C even although the porosity of activated carbon usually increased with treatment temperature and chemical concentration. Other chemicals were also used to impregnate biomass for the production of activated carbon. The activated carbon produced from Paulounia wood at a carbonization temperature of 400°C and an impregnation ratio of $ZnCl_2$ to biomass at 4:1 has a surface area of 2736 m^2/g. However, the yield of activated carbon was found to be lower than 20% when the activation temperature was at 400°C and the impregnation ratio was larger than 3:1. It was also found the impregnation ratio had a more significant effect on the porosity development than the carbonization temperature [4].

Rubber wood dust was used to produce activated carbon pellets by CO_2 activation at temperatures from 700-1000^oC [6]. The maximum surface area of the activated carbons produced was 683 m^2/g. The surface area of the activated carbon increased with the increase of activation temperature. The activated carbons produced from rubber wood dust were found to have a great potential as electrodes for super capacitors. Steam was used to activate rubber wood sawdust in a fluidized bed reactor [7]. Research was conducted to investigate the process parameters such as activation temperature, retention time, particle size and fluidizing velocity on the quality of the activated carbon. The iodine number and BET surface area of the activated carbon that was produced from the rubber wood dust with an average particle of 0.46 mm, at an activation temperature of 750°C and a retention time of 1 h were 765 mg/g and 1092 m^2/g, respectively [7].

2.1.3 Agricultural residues and by-products

Production of activated carbon from both coal and wood may compete with their other utilizations as coal is traditionally used as an energy source and woods are widely used to make furniture. Recently, agricultural residues and by-products have been investigated as promising precursors to produce activated carbons because they are abundant and renewable, have low economic value and require high disposal cost. A lot of research has been done on the production of activated carbons from agri-materials such as bagasse [8-9], coconut shell [10-11], jackfruit peel [12-13], olive stones [14-15], peach stone [16-17], rice husk/sawdust [6-7,18-19] and stalks [20].

Bagasse is a by-product of sugar production and a large amount of bagasse is generated in the sugar production process. The maximum surface area of activated carbon, which was produced from sugar beet bagasse at an activation temperature of 700°C and an impregnation ratio of $ZnCl_2$ to the biomass at 3:1, was as high as 1826 m^2/g and the total pore volume of the activated carbon was 0.966 cc/g [8]. The yield of activated carbons produced at the above conditions was 25.12%. However, the use of $ZnCl_2$ is limited due to environmental concern.

Bagasse pith, which is another waste from sugar cane industry, was also used as a precursor to produce activated carbons by both chemical activation with 28% $ZnCl_2$ and 50% H_3PO_4, and physical activation [9].

Coconut shell was investigated as a precursor to produce activated carbon [10-11]. The surface area and micro-pore volume of activated carbons produced from coconut shells char using a physical activation process were 1926 m^2/g and 0.931 cc/g, respectively. However, this physical process required high energy consumption as the physical activation temperature was up to 1000°C [10]. Microwave heating, which can significantly reduce the thermal treatment time compared to traditional heating methods, was used during physical activation of coconut shell [11].

It was found that the activated carbons produced by physical activation of coconut shell with microwave had an excellent surface area in excess of 2000 m^2/g [11]. Research also found that the CO_2 activation required longer activation time than steam or steam-CO_2 activation, and the activated carbon produced by CO_2 activation had a lower BET surface area. The comparison of porosity characterization of activated carbons by different activation agent and activation time is shown in Table 2.1 [11].

Jackfruit peel was used as a precursor to produce activated carbons at relatively low temperature of 450°C and 550°C by phosphoric acid and result in a relatively high yield of over 40% [12]. The BET surface area and total pore volume of the jackfruit peel derived activated carbon ranged from 907-1260 m^2/g and 0.525-0.733 cc/g, respectively [13].

Table 2.1. Comparison of porosity characterization and yield of activated carbons by different activation agent and activation time

Activation method	Heating method	Activation time (min)	S_{BET} (m^2/g)	V_{total} (cc/g)	V_{micro} (cc/g)	Yield (%)
Steam	Microwave	75	2079	1.212	0.9735	42.2
CO_2	Microwave	210	2288	1.299	1.012	37.5
Steam + CO_2	Microwave	75	2194	1.293	1.010	39.2

However, the surface area of the activated carbon produced from jackfruit with sulfuric acid was only 123 m^2/g. This activated carbon could effectively remove Cd (II) from an aqueous solution [13].

Fruit stones are another biomass source that can be used to produce activated carbon. It was found that the activated carbons produced from olive stones had basic surface properties and high adsorptive ability for methane blue [14]. The micro-pores contributed to more than 80% of the total pore volume of the olive stone derived activated carbon. Activated carbon has been produced from olive stones by chemical activation with KOH. It was observed that the increase in KOH concentration and decrease in stone particle size could increase the surface area of the activated carbon [15].

High quality activated carbons can also be produced from peach stones. The surface area and pore volume of the activated carbons produced from peach stones with H_3PO_4 activation at 500°C were measured at 1400 m^2/g and 0.83 cc/g, respectively [16]. The yield of the final product ranged from 40% to 43.8% depending on the concentration of phosphoric acid. The yield of the activated carbon produced from peach stones by steam activation in a fixed bed reactor at 825°C was as high as 50% [17]. It was found that the post thermal treatment of the peach stone derived activated carbon by pyrolyzing the activated carbon in nitrogen at 800°C for 1 h decreased the porosity and adsorption capability of the activated carbon for methane blue [16].

Rice husks were used to produce activated carbon in a single-stage chemical activation process at a retention time of 30 to 60 min [18]. The maximum surface area of the activated carbon was 750 m^2/g, which was obtained by impregnating the rice husks with $ZnCl_2$ at a ratio of 1:1 and a temperature of 700°C, compared to 674 m^2/g for the activated carbon produced from bagasee at an impregnation ratio of 0.75:1 and the same temperature. The surface area of the rice husk derived activated carbon was a little lower than that of the activated carbon produced from other biomass sources in literature. This might be caused by the high ash content of rice husk at 16.1%, which decreased the development of porosity in the activated carbon [19]. It was also found that the surface area of the activated carbons decreased as the increase of the temperature and retention time as the increase in activation temperature and retention time increased the formation of tar and thus prevented the porosity development [18]. Adsorption tests showed that the activated carbons produced from rice husk could remove 60%, 70% and 80% of color, COD of a landfill leachate and phenol, respectively [19].

Stalks were used to produce activated carbon in a 560 W microwave oven at an activation time of 9 min [21]. Compare to traditional heating, microwave heating can significantly shorten the activation time and reduce the energy consumption during activation. The maximum iodine number and yield of the activated carbon produced from stalks by microwave heating were 973 mg/g and 37.9%. The SEM images showed that the surface of the activated carbons had a lot of cavities that were not observed in the raw stalks. More research is needed to investigate the scaling-up of the microwave heating process for the production of activated carbon [21]. Activated carbon produced from cotton stalk has demonstrated its ability to efficiently and economically remove 2-nitroaniline dilute aqueous solution [20]. Its maximum adsorption capacity was found to be 383 mg/L at a temperature of 45°C.

2.2 Activation Methods in Activated Carbons Production

The process of preparing activated carbons can be categorized as physical activation and chemical activation. The physical activation includes carbonization of a precursor at a lower temperature in an inert gas atmosphere such as nitrogen followed by activation in oxidizing agent such as steam or carbon dioxide at a higher temperature. Chemical activation requires the impregnation of raw material with chemical reagents before thermal treatment. The most commonly used chemical reagents are $ZnCl_2$, H_3PO_4, and KOH. During chemical activation, carbonization and activation proceed simultaneously.

2.2.1 Physical activation

2.2.1.1 Process description

Physical activation includes two methods, single-step activation and two-step activation. In single-step activation, carbonization and activation of the raw materials are combined together in one process. In two-step activation, the raw materials are first carbonized in a pyrolysis process at a low temperature in an inert atmosphere such as N_2 and argon to enrich carbon content. The first step generates bio-chars and develops initial porosity. The second step is to activate the bio-char at a higher temperature with an oxidizing agent such as CO_2 or steam.

Lua et al investigated a single-step CO_2 activation process to produce activated carbons from oil palm stones [22]. Their research showed that the BET surface area of the activated carbons was significantly affected by CO_2 flow rate while the particle size of the raw material and heating rate had negligible effect on the surface area. The BET surface area slightly decreased with the increase of the heating rate. If the CO_2 flow rate increased from 25 to 200 cc/min, sufficient CO_2 will be diffused into the carbonaceous matrix and the C-CO_2 reaction produces a porous structure progressively by removing volatiles, which generates a large BET surface area.

However, if the CO_2 flow rate is too high, the C-CO_2 reaction will lead to more carbon burnt-off and the porosity destruction. Activation time and temperature also play significant roles in porosity development. At the temperature of 850°C and a retention time of 2 h, the maximum BET surface area and the micro-pore surface area were achieved at 1410 and 942 m^2/g, respectively. However, the yield of the final product at the optimum conditions was only around 15% [22].

Pistachio-nut shells were activated in a two-stage physical activation with CO_2 [23]. Research found the use of CO_2 at the second stage significantly contributed to the generation of a large surface area, compared to the use of N_2 at the second stage under the same conditions. A maximum BET surface area was 1064.2 m^2/g, which was achieved at an activation temperature of 800°C, retention time of 2.5 h, CO_2 flow rate of 100 cc/min and a heating rate of 10°C/min [23].

In recent years, single-stage physical activation has been becoming more and more popular compared to two-stage physical activation because one-step physical activation requires lower activation temperature, lower energy consumption and shorter retention time, which can reduce the production costs [24].

The carbonization itself may also include more than one stage. The char, which was obtained by a two-step carbonization process including the first stage of 400°C at a low heating rate and the second stage up to 800°C at a high heating rate of 3000°C/min, had a higher reactivity, density and mechanical strength than that carbonized by a single carbonization stage at a low heating rate. Moreover, the specific area of the activated carbons produced from the char prepared by the two-stage carbonization process was larger than that of the activated carbon prepared by the single-stage carbonization process [25].

2.2.1.2 Effect of temperature

The yield of activated carbons decreases with the increase of activation temperature as a result of the release of volatile matter, and burn-off reaction between carbon and oxidizing agent. However, the surface area and micro-porosity increase with the increase of the activation temperature. Research found that the surface area of the activated carbons prepared from coir pith by physical activation increased from 346 m^2/g to 507 m^2/g when the carbonization temperature was increased from 400°C to 800°C [26]. However, too high temperature will reduce the surface area and micro-porosity development as a result of both burn-off reaction and conversion of micro-pores to meso-pores. Activated carbons prepared from oil palm stone by one-step physical activation showed that there was a significant reduction in BET surface area and micro-pore surface area after the temperature was increased beyond 850 °C [22].

2.2.1.3 Effect of retention time

The yield of activated carbon decreases with the increase of the retention time as more and more raw materials are burnt off. The BET surface area and the micro-pore surface area increase with the retention time as micro-porosity continues to be developed over time. At the activation temperature of 890°C, the yield of the activated carbons prepared from tar pitch by CO_2 activation decreased from 80% to 6% when the activation time was increased from 3 h to 22.5 h. Meanwhile, the total pore volume increased from 0.29 to 0.86 cc/g and the BET surface area increased from 644 to 2487 m^2/g [27]. However, too long retention time will reduce the BET surface area, total pore volume and micro-pore surface area due to severe burnt-off phenomenon between carbon and oxidizing agent, and the conversion of micro-pores to meso-pores and macro-pores [22].

2.2.1.4 Effect of activating agent

Aworn [28] conducted a study on the effect of activating agents on the development of micro-pore and meso-pore of activated carbons prepared from agricultural wastes such as nut shell, corncob char and bagasse bottom ash. His research showed that for all materials, steam activation generated larger meso-pore volume and lower micro-pore volume than CO_2 activation because the CO_2 activation creates micro-pores while steam activation enlarges the micro-pores into meso-pores and thus generate less surface area during the activation process. In terms of the application of activated carbons, activated carbons produced from bagasse bottom ash and sawdust dust with more meso-pores can be used to adsorb large molecules [29].

The combination of two activation agents may lead to better porosity development than an individual agent. Activated carbons prepared from three types of coals showed that the combination of CO_2 and steam in the activation process resulted in larger surface area than either CO_2 or steam used alone [29]. This may be because steam can widen the micro-pores to give new sites for CO_2 to develop new micro-pores. It was also found the activation with CO_2-steam and CO_2 could develop more uniform pores than steam [29].

2.1.1.5 Effect of flow rate

The flow rate of activating agents has a significant effect on porosity development of activated carbons. At an activation temperature of 650°C, the BET surface area increased slightly as the CO_2 flow rate was increased [22]. However, as the activation temperature was increased from 650 to 850°C, the BET surface area increased dramatically as CO_2 flow rate increased from 25 to 100 cc/min while the porosity decreased with the increase of the CO_2 flow rate at this temperature. If the flow rate of CO_2 was further increased up to 200 cc/min, there was a detrimental effect on porosity development as a result of the severe burnt-off effect [22]. Another research also confirmed that the optimum flow rate of CO_2 was 100 cc/min to produce activated carbons with the largest surface area at 800°C for 2 h [23].

2.2.1.6 Effect of heating rate

The effect of heating rate on the porosity development and yield of activated carbons is not as significant as temperature and retention time. Typical heating rates are 5°C/min and 10°C/min during the carbonization and activation process although the heating rate varies from 2 to 300°C/min [22-23, 25-36]. However, heating rate may have an effect on the micro-porosity development in the physical activation process. Research showed that as the heating rate increased from 5°C/min to 20°C/min, the change of the BET surface area was not significant. However, the micro-pore surface area was reduced from 936 m^2/g to 852 m^2/g as the heating rate increased from 5°C/min to 20°C/min [22].

2.2.2 Chemical activation

2.2.2.1 Process description

Activated carbons can also be produced by chemical activation, in which the precursors are impregnated with chemicals such as KOH, H_3PO_4, and $ZnCl_2$ and then carbonized in an inert atmosphere such as N_2. During chemical activation, carbonization and activation of the raw materials usually proceed simultaneously.

H_3PO_4 is widely used to produce activated carbon from biomass. Budinova [37] conducted a research on the production of activated carbons from woody biomass by H_3PO_4 activation at 600°C in an inert atmosphere. It was found that the increase of the concentration of H_3PO_4 from 20% to 50% increased the adsorptive capacity of the activated carbon by 30%. The replacement of the inert gas with steam could improve the porosity development because the combination of both physical activation and chemical activation was a favorable method to produce high quality activated carbons [37].

A separate carbonization and activation process was also used to prepare precursors for the further chemical activation. Different purging gases were used to prepare precursors at a temperature of 500°C for 2 h before the impregnation with 50% H_3PO_4 [38]. It was found that the purging gas of air could generate an activated carbon with the largest surface area [38].

$ZnCl_2$ is another chemical widely used in chemical activation. The surface area of the activated carbon, which was produced from pomegranate seeds by chemical activation with $ZnCl_2$ at an impregnation ratio of 2 and a carbonization temperature of 600°C, was 978.8 m^2/g [39]. It was also found that the yield of the activated carbon produced by chemical activation was higher than that of bio-chars produced at the same carbonization temperature [39].

Another research showed that the BET surface area of the activated carbon carbons prepared from cherry stones by chemical activation with $ZnCl_2$ at an impregnation ratio of 4 was 1971 m^2/g [40]. Research found that the increase in impregnation ratio had more effect on the development of the porous structure than the increase in carbonization temperature. However, the increase in carbonization temperature had more effect on the functional groups of pore surface than the increase in impregnation ratio [40].

KOH is also widely used as an activating agent in activated carbons production. Sudaryanto [41] conducted research on the production of activated carbons from cassava peel by a single stage KOH activation, in which the raw material was impregnated with KOH, and carbonized and activated simultaneously. The single stage activation process can reduce the energy consumption. The single stage KOH activation process did not include the step of low-temperature carbonization to produce bio-chars for the further impregnation with KOH. The maximum surface area of 1605 m^2/g was obtained at 750°C with an impregnation ratio of 5:2 for 1 h.

The combination of KOH activation and CO_2 activation is an effective way to produce high surface area activated carbons from pistachio shells. It was found that KOH activation at 780°C for 60 min followed by CO_2 gasification at the same temperature for 30 min produced activated carbons with the highest surface area of over 1900 m^2/g and best adsorptive properties as a result of significant proportion of meso-pores [42].

The production of activated carbon with KOH activation usually involves two steps, including the carbonization of raw materials to produce bio-chars, which are rich in carbon content and have rudimentary pores; and the activation of the bio-chars, which are impregnated with KOH and activated at a higher temperature. Tseng [43] conducted research on the porosity development and adsorption performance of the activated carbons produced from corncob by two-stage KOH activation. Activated carbons prepared from corncob at an impregnation ratio from 0.5 to 2 had a BET surface area from 841 to 1221 m^2/g. It is possible to achieve much higher surface area from 1976-2595 m^2/g at higher impregnation ratios. The scan electric microscope (SEM) images showed the impregnation ratio had a significant effect on the surface morphology of honeycombed holes of activated carbons produced from corncobs with KOH [43].

2.2.2.2 Effect of temperature

Temperature has a significant effect on both yield and porosity development of activated carbons by chemical activation. As the temperature increases, more volatile matters and gaseous products are released from the carbonized materials, which decreases the yield of the final products [12, 44-45]. As temperature increases within a certain range, the surface area of activated carbon increases because of the promotion of dehydration and degradation at higher temperatures which develop more pores. However, too high temperature will decrease the surface area as a result of the transformation of micro-pores to meso-pores and disappearance of some pores which are damaged at a high temperature [45-47].

2.2.2.3 Effect of retention time

As the retention time increases, the yield of the activated carbons decreases as a result of the increase in a total weight loss caused by dehydration and degradation. On the other hand, the surface area of the activated carbons increases as the increase of the retention time because the degradation and dehydration continue to develop pores. However, too long retention time decreases the surface area because more and more micro-pores are changed to meso-pores and burnt-off [46, 48].

2.2.2.4 Effect of impregnation ratio

The impregnation ratio of chemicals is considered as one of the most critical factors in developing porosity of carbon materials during chemical activation. As the impregnation ratio increases, the excess of chemicals will promote gasification of the carbonized materials and decrease the yield of activated carbons. On the other hand, the increase of the impregnation ratio within a range can significantly help to develop porosity. However, the further increase of the impregnation ratio beyond a certain level, the pore size distribution might be changed and more larger pores will be generated, which reduces the surface area and pore volume of the activated carbon [43, 46].

2.2.2.5 Effect of flow rate and heating rate

During chemical activation, carbonization and activation of the impregnated raw materials proceed under the protection of inert gases such as nitrogen or argon. Various literatures showed the flow rate of inert gases is not a significant factor on the porosity development of the activated carbons produced by chemical activation. A nitrogen flow rate at 150 to 300 cm^3/min is most widely used for the activated carbons production while a higher flow rate at 2 to 4 dm^3/min are also used [30-49]. Heating rate is also a fixed parameter at 5 °C/min and 10 °C/min in most research on activated carbon production [30-50].

2.2.3 Comparison between physical and chemical activation

Research has also been done on comparison of the advantages and disadvantages of physical and chemical activation. Activated carbons were prepared from coal tar pitch by both physical and chemical activation [27]. The results showed two disadvantages of physical activation. First, physical activation generated a much lower yield of 6% when the surface area was around 2500 m^2/g compared to 47% when the surface area was almost the same by chemical activation. Second, the surface of the final product was more damaged when physical activation was applied. Comparison of porosity properties and yield of activated carbon by different activations is summarized in Table 2.2.

Table 2.2. Comparison of porosity properties and yield of activated carbon produced by physical and chemical activation

Activation method	**S_{BET} (m^2/g)**	**V_{total} (cc/g)**	**Yield (%)**	**Reference**
Chemical (KOH)	2420	0.94	47	[27]
Physical (CO_2)	2487	0.86	6	[27]
Chemical (KOH)	2270	1.21	22	[51]
Physical (CO_2)	2220	1.10	12	[51]

Similar results were found in Teng's research on the activated carbons produced from phenol-form-aldehyde resins by both chemical and physical activation [51]. It was found that high-porous activated carbons could be produced by chemical activation with KOH impregnation and physical activation with CO_2. To obtain similar porosity properties, yield of activated carbon produced by physical activation was found to be lower than that produced by chemical activation.

2.3 Application of Activated Carbons

Activated carbons have already found many applications such as air pollution control [52], removal of acid dyes [53-56], wastewater and groundwater treatment [57-59], removal of heavy metals [55-56], removal of phenols [60-61], removal of mercury vapors and volatile organic compounds [62-63]. Activated carbons have very high adsorption capacity due to their high surface area and pore volume. Generally speaking, activated carbons with basic surface chemical properties are appropriate for the adsorption of acidic gases such as sulfur dioxide while activated carbons with acidic surface chemical properties are good at the adsorption of basic gases [64].

2.3.1 Waste water treatment

Activated carbons have been used to remove chemicals in waste water. Activated carbons prepared from sawdust and rice husk are economically feasible to remove an acid dye (Acid Yellow 36) from waste water [53]. One gram of the activated carbons produced from sawdust and rice husk could adsorb 183.8 mg and 86.9 mg of the acid dye from an aqueous solution at a pH value of 3, respectively.

Ricordel [56] conducted research on the kinetics of adsorption of heavy metals such as Pb^{2+}, Zn^{2+}, Ni^{2+} and Cd^{2+} at an initial ion concentration of 0.15 mM by activated carbons prepared from peanut husks. The results showed the adsorption performance was significantly affected by particle size distribution of the activated carbon and the carbon to metal ratio.

Activated carbon column prepared from pistachio shell by H_3PO_4 activation was investigated to recover valuable aroma from waste streams [57]. It was found that the removal rates of aroma from three waste water sources were very high from 44% to 99%. Also, this process did not require any heat treatment that might damage the structure of aroma. Activated carbon would not change the chemical structure or property of the aroma recovered.

2.3.2 Gas storage

A lot of research has been conducted on gas storage by activated carbons [65-68]. Biloe [65] designed an activated carbon adsorption system to store natural gas. It was found that the appropriate micro-pore sizes of activated carbons must be, on average, 1.5 nm and 2.5 nm respectively for the adsorption and desorption of natural gas. The investigation of relationship between micro-porosity and hydrogen storage capacity showed that the pure carbonaceous structure of the activated carbon was not suitable for hydrogen storage while an upper limit of 4% hydrogen storage could be achieved by activated carbons with a micro-pore volume from 0.35 to 0.45 ml/g [67].

Research has been conducted on the performance of hydrogen storage by both advance activated carbon monoliths and activated carbon [68]. It was shown that hydrogen can be highly adsorbed only when the two materials have large micro-pore volume and high packing density. Advanced activated carbon monoliths prepared under the optimized conditions have excellent mechanic properties and can achieve an outstanding hydrogen adsorption capacity of 29.7 g H_2/l at 77 K and 4 MPa.

2.3.3 Catalyst support

Activated carbon can also be used as a catalyst support such as Palladium catalysts and ammonia synthesis catalysts [69-70] because activated carbon has a large surface area and high adsorptive capability. Kang et al. [71] studied the effect of heat treatment during activation process on the structural and electronic properties of the activated carbon to be used as a catalyst support. Their research showed that the catalytic activity could be mainly attributed to the well-loaded Pt_0 catalyst. The catalytic activity of Ba-promoted Ru catalyst on activated carbon for the ammonia synthesis was significantly increased when activated carbons was heated at 1900°C in an inert atmosphere and oxidized before they were used as the catalysts support [69].

2.3.4 Other application

Activated carbon can also be used in many other areas such as medical care and food industry. Some potential applications are summarized in Table 2.3.

Table 2.3. Other applications of activated carbon

Other applications	Example
Air purification	Indoor air purification [72]
	H_2S removal from moist air streams [73]
Medical care	Silver recovery from X-ray process effluents [74]
	Extracorporeal therapies [75]
Gas purification	Flue gas purification [76]
Food industry	Vinegar decolorization [77]

2.4 Conclusions

Activated carbons are traditionally produced from coal and woody biomass. Agricultural residues and by-products are potential, cheap, abundant and renewable alternatives to coal and woody biomass to make activated carbons [6-20]. Moreover, the agricultural materials have a high carbon content and low ash content that are favorable characteristics of a material for activated carbon production.

Activated carbon can be produced by either chemical activation or physical activation. Physical activation does not require input of chemicals which can reduce the cost of downstream purification. However, physical activation requires higher temperature and energy consumption while the yield of activated carbon is lower than that of chemical activation.

On the other hand, chemical activation can produce activated carbon with higher surface area and pore volume given the yields of activated carbon from both activation methods are the same. Physical activation and chemical activation can be combined to produce high quality activated carbon.

Activated carbon have been applied in many environmental areas such as waste and ground water remediation, control of air pollution and recovery of valuable components from water streams. Due to the large surface area and pore volume, activated carbon is also used as a vehicle for gas storage such as hydrogen storage and methane storage. Activated carbon becomes a more and more popular supporting material in catalyst development in chemical industry.

CHAPTER 3

MATERIALS AND METHODS

3.1 Raw Material for Activated Carbon Production

Although a lot of research has been done on preparation of activated carbon from different varieties of raw materials by various activation methods, there is still little information on the production of activated carbons by residues from biorefinery processes such as fermentation and pyrolysis processes. Fermentation residues are usually discarded as wastes or dried and burned in a boiler for heat supply, which adds the limited or negative amount of economic value and may create damage to the environment and ecological system. The bio-char from a pyrolysis process is usually used to improve the quality of soil. If those residues can be developed as activated carbons which have found many applications in various industries, both fermentation and pyrolysis industries would make profits from the upgraded by-products of activated carbons while minimizing the negative environmental impacts of these residues.

Raw materials for the production of activated carbons in this study included fermentation residues, pyrolysis residues and agricultural residues.

3.1.1 Fermentation residues

Fermentation residues were collected from the bio-processing lab at North Carolina Agricultural and Technical State University.

Two kinds of fermentation residues were collected and they are:

- Residues collected from simultaneous saccharification and fermentation of switch grass which was pretreated by four different ways:

(1) hot water pretreatment at 180°C

(2) 10% acetic acid pretreatment

(3) 10% acetic acid pretreatment and $CaCO_3$

(4) $Ca(OH)_2$ or lime pretreatment.

Conditions of simultaneous saccharification and fermentation from switch grass are summarized in Table 3.1.

Table 3.1. Conditions of simultaneous saccharification and fermentation from switch grass

Temperature (°C)	Time (day)	pH	Enzyme loading
30	7	4.9	15 ml/g glucan 50 ml/g hemicellulase 1 g/L Saccharomyces cerevisiae

- Residues collected from separated hydrolysis and fermentation of five different biomass including switch grass, wheat straw, cattail, corn stover and sorghum, which were pretreated by four different ways:

  (1) 90°C water plus 5% acetic acid

  (2) 90°C water plus 10% acetic acid

  (3) 180°C water plus 5% acetic acid

  (4) 180°C water plus 10% acetic acid

Conditions of separated hydrolysis and fermentation are summarized in Table 3.2.

After the fermentation process was completed, the solid residues were decanted from fermenters and centrifuged by at 20°C and rotation rate of 3000 rpm for 15 min. The residues were then decanted from the centrifuge tubes and dried in an air circulated oven at 105°C for 12 h for the further production of activated carbon. Conditions of separated hydrolysis and fermentation are shown in Table 3.2.

Table 3.2. Conditions of separated hydrolysis and fermentation

	Temperature (°C)	**Time (day)**	**pH**	**Enzyme loading**
Hydrolysis	50	7	4.9	15 ml/g glucan 50 ml/g hemicellulase
Fermentation	30	7	4.9	1 g/L Saccharomyces cerevisiae

3.1.2 Pyrolysis residues

Pyrolysis residues were collected from pyrolysis reaction of various agricultural biomass, including switch grass corn stover and wheat straw.

The conditions of pyrolysis process are as follows:

- Pyrolysis temperature: 450°C
- Residence time: 1 h
- N_2 flow rate: 500 cc/min
- Heating rate: 10°C/min

Those residues were washed with de-ionized water and dried in an air circulated oven at 103°C for 12 h for the further production of activated carbon.

3.1.3 Agricultural residues

Agricultural residues include raw biomass of switch grass, wheat straw and corn stover. Wheat straw and corn stover were obtained from the university farm at North Carolina Agricultural and Technical State University. Switch grass was collected from the farm of Purdue University. The biomass materials were ground to pass a 1 mm screen with a laboratory mill (Wiley Mill Model 4, Thomas Scientific, NJ). These residues were washed with de-ionized water and dried in an air circulated oven at 103°C for 12 h.

3.2 Elemental Analysis of Various Residues

The elemental analysis of the biomass materials was conducted on a Perkin Elmer 2400 Series II CHNS/O Analyzer. CHN mode, which is the most universal mode for elemental analysis, was chosen as the analysis option, because in this mode the reagent design is combined and different combustion control parameters are optimized. In this analysis mode, main interfering elements such as sulfur and halogen are already removed so that oxygen content is calculated as:

$$O\ (\%) = 1 - C\ (\%) - H\ (\%) - N\ (\%)$$

In this study, samples at size from 0.5 to 2 mg were weighed in Perkin Elmer tin capsules (5 x 8 mm) solids using an ultra microbalance. The samples in capsules were then loaded to the auto sampler of Perkin Elmer 2400 Series II CHNS/O Analyzer, for which automatic sample injection mode was applied so that up to 60 samples could be injected automatically at one time. It takes 6 min for the CHN analysis mode to analyze.

3.3 Ash Analysis of Various Residues

Ash content of a biomass material is very important property to determine if it is appropriate as a precursor for the production of high quality activated carbon. Ash in biomass materials will form tars during the activation process at a high temperature and prevent porosity development in activated carbon.

Ash content is defined as inorganic residues left in materials after dry oxidation at 575°C for a given time period.

In this study, 3 g of biomass materials were burned in crucibles in a muffle furnace at 575°C for 4 h. The ash content was calculated as the residues after the oxidation divided by the original weight of the biomass, which was 3 g in this study.

3.4 Production of Activated Carbon from Fermentation Residues

Fermentation residues which were collected from simultaneous saccharification and fermentation of switch grass pretreated by 10% acetic acid were used for the production of activated carbon.

Fermentation residues were dried in an air circulated oven at 103°C for 12 h to remove moisture.

Each 3 g sample of dried fermentation residues was weighed and soaked with 6 g phosphoric acid at concentrations of 10%, 20% and 30% at room temperature for 12 h.

Then these impregnated fermentation residues were moved and kept in an air circulated oven at 103°C for 12 h to remove water.

One stage of carbonization/activation was used to produce activated carbon from fermentation residues. During carbonization/activation, the impregnated fermentation residues with phosphoric acid at different concentrations were placed in a muffle furnace and heated up to 450°C, 550°C and 650°C for 1 h and 2 h at a heating rate of 10°C/min. The carbonization/activation process was performed under the protection of the nitrogen gas at a flow rate of 500 ml/min.

After the carbonization/activation process was finished, all of the activated carbon products were repeatedly washed with hot de-ionized water at 70°C until constant pH of the solution was reached. Then these activated carbons were dried in a vacuum oven at 103°C for 12 h. The activated carbons were then stored in desiccators for future analyses such as BET analysis.

Thermal gravimetric analysis (TGA) was used to determine the dynamic weight loss of different residues impregnated by different chemicals during the carbonization/activation process.

All samples of fermentation residues impregnated with phosphoric acid were heated up to 450°C, 550°C and 650°C at a heating rate of 10°C /min and held at the final temperatures for 3 h under the protection of nitrogen.

3.5 Production of Activated Carbon from Pyrolysis Residues

As residues produced from pyrolysis process are already rich in carbon content and have developed the rudimentary porosity, KOH activation was used for the activated carbon production from pyrolysis residues. Each 3 g sample of pyrolysis residues was weighed and was soaked with 6 g KOH solution at room temperature for 12 h.

These impregnated pyrolysis residues were moved and kept in an air circulated oven at 103°C for 12 h to remove water.

One stage of carbonization/activation was used for the production of activated carbon from pyrolysis residues. These impregnated pyrolysis residues were placed in a muffle furnace and heated up to 780°C for 1 h at a heating rate of 10°C/min. The carbonization/activation process was performed under the protection of the nitrogen gas at a flow rate of 500ml/min.

After the carbonization/activation process was finished, all of the activated carbon products were repeatedly washed with hot de-ionized water at 70°C until constant pH of the solution was reached. Then these activated carbons were dried in a vacuum oven at 103°C for 12 h. The activated carbons were then stored in desiccators for future analyses such as BET analysis.

3.6 Production of Activated Carbon from Agricultural Residues

Activated carbon was prepared from switch grass by phosphoric acid. The conditions of the production process were same as the optimized conditions obtained from the production process for fermentation residues.

3.7 Analysis of BET Surface Area and Pore Volume

For this purpose, the characterization of the pore structure and surface area of the activated carbons produced from different varieties of precursors were determined by nitrogen adsorption at 77 K using a Quantachrome NOVA 2200.

Before the nitrogen adsorption was carried, all of the activated carbon samples were degassed in a vacuum at 300°C for 3h.

Nitrogen adsorption isotherms were measured from liquid nitrogen uptake over a relative pressure (P/Po) range from approximately 0.05 to 0.95, which were used to determine different porosity properties including BET surface area, total pore volume, micro-pore and meso-pore volume. The BET surface area was calculated by means of the standard Brunauer–Emmett–Teller equation applied in the relative pressure range from 0.05 to 0.35. The total pore volume was assessed by liquid nitrogen adsorption at a P/P_0 = 0.95 at which all pores are considered to be completely filled with liquid nitrogen. The micro-pore volume was determined by cumulative pore volume from pore size distribution. The density function theory was used to calculate the pore size distribution of all activated carbon samples by nitrogen adsorption isotherms at 77 K, using Quantachrome software. The meso-pore volume was determined by subtracting micro-pore volume from total pore volume.

3.8 Catalyst Development with Activated Carbon

3.8.1 Preparation of activated carbon catalyst support

Activated carbons prepared from agricultural residues (ACA) and activated carbons prepared from pyrolysis residues (ACP) were used as supporting materials for catalyst development. All ACA and ACP were washed with 2 M HCl solution under reflux for 12 h in order to remove ash and sulfur, followed by being washed by de-ionized water under reflux for 6 h. Then the washed supporting materials were dried in an air circulated oven at 105°C for 12 h. After that, the dried supporting materials were evaluated at 300°C in a muffle furnace under the flow of nitrogen gas for 12 h.

3.8.2 Preparation of catalysts supported on activated carbon

Catalysts were prepared by incipient wetness impregnation of the activated carbons by iron nitrate ($Fe(NO_3)_3{\cdot}9H_2O$) aqueous solution. Iron nitrate aqueous solution was prepared so that the concentration of iron element was 1%. The aqueous solution was stirred on a magnetic/heat plate at a speed of 1000 rpm or even higher. These pretreated supporting materials were added into the iron aqueous solution as slowly as possible. The load ratio of iron aqueous solution to activated carbon was 15 ml/g. The iron aqueous solution with added activated carbons was kept being stirred for 2 h with the same stirring speed. Then the catalysts were filtrated out of the aqueous solution and dried in an air circulated oven at 105°C for 12 h. Finally, the catalysts on the activated carbon support were calcinated in a muffle furnace at 450°C under nitrogen flow protection for 3 h.

3.8.3 Characterization of catalysts

Nitrogen adsorption isotherms of catalysts supported on activated carbon prepared from various residues were measured using a Quantachrome NOVA 2200 at 77 K.

3.8.4 Thermal gravimetric analysis (TGA) of catalysts

The stability of iron nitrate catalysts supported by activated carbons from different residues was tested by TGA analysis. Those catalysts were heated up to 200°C at a heating rate of 10°C/min in air for 2 h.

3.9 Statistical Analysis

Replicates of experiments were done on randomly selected samples in order to test if results were compatible and relative standard deviation was within an acceptable range.

A 3×3×2 factorial design (Table 3.3) was used in optimization of activated carbon produced from fermentation residues. Regression analysis was conducted in Microsoft Excel. Regression analysis was done to fit the response function (Yield, BET surface area and Total pore volume).

The factorial model that was used to fit the data obtained from experiments is:

$$Y = a_0 + a_1x_1 + a_2x_2 + a_3x_3 + a_{12}x_1x_2 + a_{13}x_1x_3 + a_{23}x_2x_3 + a_{123}x_1x_2x_3$$

Table 3.3. Values of operating variables used in the designed set of experiments

	x_1 (Activation temperature) (°C)	**x_2 (Phosphoric acid concentration) (%)**	**x_3 (Activation time) (h)**
Level 1	450	10	1
Level 2	550	20	2
Level 3	650	30	N/A

3.10 Economic Analysis

3.10.1 Flow diagrams of the processes for producing activated carbon from fermentation and pyrolysis residues

Flow diagrams of the processes for producing activated carbon from fermentation and pyrolysis residues are given in Figures 3.1 and 3.2. These flow diagrams are used to determine the equipment size and material and energy flows in the facilities of manufacturing activated carbons from fermentation and pyrolysis residues for economic analysis.

The main assumptions for the process used to produce activated carbon from fermentation and pyrolysis residues are:

- H_3PO_4 solution is used to impregnate fermentation residue at a mass ratio of 2:1
- About 60% of H_3PO_4 is recovered through condensation
- The processes are operated at conditions determined by this research

The main assumptions for the process used to produce activated carbon from pyrolysis residues are:

- KOH solution is used to impregnate fermentation residue at a mass ratio of 2:1
- About 85% of KOH is recovered through condensation
- The processes are operated at conditions determined by this research

The main units of this facility include soaking tank for impregnation, rotary drier for drying raw material and products, rotary kiln for activation process, washing tank, storage tank and condenser.

The basic processes for producing activated carbons from these two facilities are simplified and very much similar to lab experiment process of activated carbon production. The only difference between the two processes is fermentation residues need drying before they are impregnated with chemicals. Therefore, one more step of drying is needed which increase the capital cost given other units are the same.

Fermentation residues

H_3PO_4 soak
tank
(Impregnation)

Rotary
drier

Rotary kiln
450°C 1h
(Activation)

H_3PO_4

H_3PO_4
storage tank

Condenser
70% recovered
H_3PO_4

5000 L
Washing
tank

Activated carbon

Storage tank for
activated carbon

Rotary drier

Figure 3.1 Flow diagram of the process for production of activated carbon from fermentation residues

Pyrolysis residues

KOH soaking
tank
(Impregnation)

Rotary
drier

Rotary kiln
780°C 1h
(Activation)

KOH

KOH
storage tank

Condenser
70% recovered
KOH

Washing
tank

Activated carbon

Storage tank for
activated carbon

Rotary drier

Figure 3.2 Flow diagram of the process for production of activated carbon from pyrolysis residues

3.10.2 Capital costs

Capital cost is usually a function of the capacity or the scale of a facility. The power function is a common estimation function to determine capital cost at different scales. The capital costs of each component in the facilities were calculated by the power function:

$$\frac{C_{p,s}}{C_{p,b}} = \left(\frac{S_s}{S_b} \right)^n$$

where

$C_{p,s}$ = estimated cost of the equipment at a specific size

$C_{p,b}$ = known cost of the baseline equipment

S_s = size of the specified equipment

S_b = size of the baseline equipment

n = economy of scale sizing component

Typically, the economy of scale sizing component is from 0.6 – 0.8. In this study, the power factor set at 0.6. The equipment costs at reference scales and other associated cost were obtained from various literature [78-83].

The capital costs consist of equipment costs, and installation costs and indirect costs associated with the installation. The installation and indirect costs were calculated as percentages of the equipment costs. Specifically, installation and indirect costs were given in Table 3.4.

3.10.3 Operating costs

The operating costs include the costs for biomass feedstock, activating chemicals, utilities, labor, maintenance, supplies, taxes, insurance and general expenses. Summary of operating cost are shown in Table 3.5.

Table 3.4. Summary of capital costs

Capital costs	**Calculation**
Direct project expenses	
Equipment	C_P
Materials for installation	C_M = MMF x C_P
Direct labor	C_L = LMF x (Cp + C_M)
Total direct	$C_D = C_P + C_M + C_L$
Indirect project expenses	
Freight, insurance, taxes	$C_{FIT} = 0.08C_P$
Construction overhead	$C_O = 0.7C_L$
Engineering expenses	$C_E = 0.15 (C_P + C_M)$
Total indirect	$C_{ID} = C_{FIT} + C_O + C_E$
Bare module cost	$C_{BM} = C_D + C_{ID}$
Contingency & fee	$C_{CF} = 0.18C_{BM}$
Total module cost	$C_{TM} = C_{BM} + C_{CF}$
Auxiliary facilities	$C_{AF} = 0.3C_{TM}$
Total capital	$T = C_{TM} + C_{AF}$

The raw material cost of fermentation residues was considered to be 0 since this facility was intended to be set up along with the fermentation facility. Therefore, the cost of fermentation residues is only calculated as the cost of drying those residues which has be included in the equipment cost.

Table 3.5. Summary of operating costs

Item	Calculation
Fermentation/pyrolysis residues	0 ($114/kg)
H_3PO_4 (KOH)	$1/kg ($2.5/kg)
Utilities ($/d)	649/749
Operating labor	3 shifts/d, 20$/h
Supervisory labor	15% of operating labor
Maintenance & repairs	5% of total capital
Supplies	15% of Maintenance & repairs
Taxes	1% of total capital
Insurance	0.5% of total capital
General expenses	15% of operating labor
Annual capital charges	$C_{total}\ i\ (1+i)^n/[(1+n)^n - 1]$
Anual operating cost	Sum of the items above
Production cost ($/kg)	Annual operating cost divided by annual production output

The costs of pyrolysis residues, phosphoric acid and potassium hydroxide were either obtained from literature [78-83].or quotes. Utilities costs were also estimated from literature. It was also assumed the facility is operated for 350 d/yr, 3 shifts/day, 24 h/d.

The daily processing capabilities associated with the number of persons per shift are shown in Table 3.6.

Table 3.6. Daily processing capability associated with number of person per shift

Daily processing capability (kg)	**3000**	**5000**	**7000**	**9000**
Number of person per shift	2	4	6	8

Interest rate is set to be 10% and the operation time of the facility is assumed to be 15 years. The total annual production costs include the annualized capital cost and annual operating costs. The production cost per kg of activated carbon was calculated by dividing the total annual production costs by the annual production capacity.

CHAPTER 4

RESULTS AND DISCUSSION

4.1 Elemental Analysis of Different Residues

Elemental analysis of agricultural, fermentation and pyrolysis residues were given in Table 4.1. It can be seen from Table 4.1 that the five raw agricultural residues of wheat straw, corn stover, switch grass, sorghum bagasse and cattail have carbon contents from 39.89 to 47.33%.

Fermentation residues from separated hydrolysis and fermentation (SHF) of different agricultural residues pretreated by 10% acetic acid have similar carbon content to those of raw agricultural residues. However, chemical used for during the pretreatment of biomass affected the elemental compositions of fermentation residues. The fermentation residues from switch grass pretreated with alkaline such as $Ca(OH)_2$ and $CaCO_3$ have much lower carbon content than that of the raw switch grass. This is because that an alkaline solution can remove lignin from biomass during pretreatment and lignin has higher carbon content than those of other biomass components of cellulose and hemicellulose. Alkaline also react with the organic acids with biomass to generate salts in the pretreated biomass, which decreases the percentage of organic matter in the pretreated biomass as shown in Table 4.2. Fermentation residues with a high carbon content are suitable to be used as precursors to prepare activated carbons. As shown in Table 1, the carbon contents of pyrolysis residues at 66-67% are much higher than those of raw agricultural residues at around 45%.

Table 4.1. Elemental analysis of agricultural, fermentation and pyrolysis residues

	Biomass	Elemental analysis			
		C (%)	H (%)	O (%)	N (%)
Agricultural residues	Wheat straw	43.11	4.93	51.38	0.58
	Corn stover	43.42	5.45	50.50	0.63
	Switch grass	47.33	5.71	46.21	0.75
	Sorghum bagasse	39.89	5.08	53.65	1.38
	Cattail	47.56	5.75	45.46	1.23
Residues from SHF of biomass pretreated by 10% acetic acid solution at 180°C	Wheat straw	46.02	6.14	47.33	0.51
	Corn stover	45.34	6.54	47.22	0.90
	Switch grass	44.95	6.01	48.33	0.71
	Sorghum bagasse	43.84	7.02	48.3	0.84
	Cattail	48.82	6.81	42.88	1.49
Residues from SSF of switch grass pretreated by different methods	H_2O	45.05	5.58	48.49	0.88
	Acetic acid	44.76	5.58	48.89	0.77
	$Ca(OH)_2$	34.09	4.08	60.39	1.44
	Acetic acid/$CaCO_2$	40.22	4.71	54.12	0.95
Pyrolysis residues	Wheat straw	66.97	2.06	30.27	0.70
	Corn stover	66.52	2.10	29.87	1.51
	Switch grass	66.19	2.83	29.92	1.06

These differences of carbon content among the agricultural, fermentation and pyrolysis residues indicate that a fermentation process does not significantly change the elemental composition of the raw agricultural residues while a pyrolysis process burns off most of the volatile materials in the raw agricultural residues by dehydration and degradation and significantly enrich the carbon content of the final product of pyrolysis residues.

4.2 Ash Analysis of Different Residues

Ash and moisture of agricultural, fermentation and pyrolysis residues were given in Table 4.2.

As shown in Table 4.2, all residues have ash content lower than 15%, which might not affect the porosity development during activation process and can be considered as appropriate precursors for activated carbon production. Fermentation residues with raw materials pretreated by either hot water or acetic acid or both combined have lower ash content than their raw agricultural residues. Some ash in the raw agricultural residues is washed away during the pretreatment with acetic acid or hot water, hydrolysis and fermentation. However, fermentation residues with raw materials pretreated with alkaline have higher ash content that their raw agricultural residues because alkaline react with the organic acids in biomass to generate salts in the pretreated biomass, which increases the ash content in the fermentation residues.

Pyrolysis residues have ash content higher than 11%, which is much higher than those of raw agricultural residues. This is because during the pyrolysis process a lot of the volatile matters are released at a high temperature while all ash is left in the bio-char, which concentrate the ash content in the pyrolysis residues.

Table 4.2. Ash and moisture content of agricultural, fermentation and pyrolysis residues

	Biomass	**Ash (%)**	**Moisture (%)**
Agricultural residues	Wheat straw	9.33	1.18
	Corn stover	6.38	1.44
	Switch grass	4.15	1.24
	Sorghum bagasse	10.74	1.36
	Cattail	7.65	1.25
Residues from SHF of different biomass pretreated by 10% acetic acid/180℃ H_2O	Wheat straw	8.99	1.13
	Corn stover	5.22	0.92
	Switch grass	3.87	1.05
	Sorghum bagasse	9.95	0.98
	Cattail	7.25	1.32
Residues from SSF of switch grass pretreated by different methods	H_2O	3.82	1.45
	Acetic acid	3.91	1.38
	$Ca(OH)_2$	8.05	1.52
	Acetic acid/$CaCO_3$	7.95	1.11
Pyrolysis residues	Wheat straw	12.36	0.05
	Corn stover	11.27	0.06
	Switch grass	11.20	0.06

4.3 Production of Activated Carbon from Fermentation Residues

4.3.1 Effect of temperature on yield of activated carbon from fermentation residues

Figure 4.1 and 4.2 show the effect of activation temperature on the yield of activated carbons. It can be seen that the yield of activated carbon decreases when the activation temperature increases from 450°C to 650°C and held at the final temperature for 1 h and 2 h for all samples impregnated with phosphoric acid at different concentrations from 10% to 30%. Higher temperatures are more favorable for phosphoric acid as a catalyst to promote dehydration and degradation of biomass, which release the volatile matters from the impregnated fermentation residues and decrease the yield of the activated carbon. Gasification reaction is also enhanced at higher temperatures, which releases the gaseous products from the biomass and decrease the yield of the activated carbon.

As shown in Figure 4.1, if the activation temperature increased from 450°C to 550°C, the yield of the activated carbon decreased sharply. If the activation temperature was further increased 550°C to 650°C, the yield of the final activated carbon decreased slightly.

4.3.2 Effect of phosphoric acid concentration on yield of activated carbon from fermentation residues

The effect of phosphoric acid concentration on the yield of final product of activated carbon is shown Figure 4.3 and Figure 4.4. It can be seen in Figure 4.3 that for the yields of final product of activated carbon decrease as the phosphoric concentration increases from 10% to 30%.

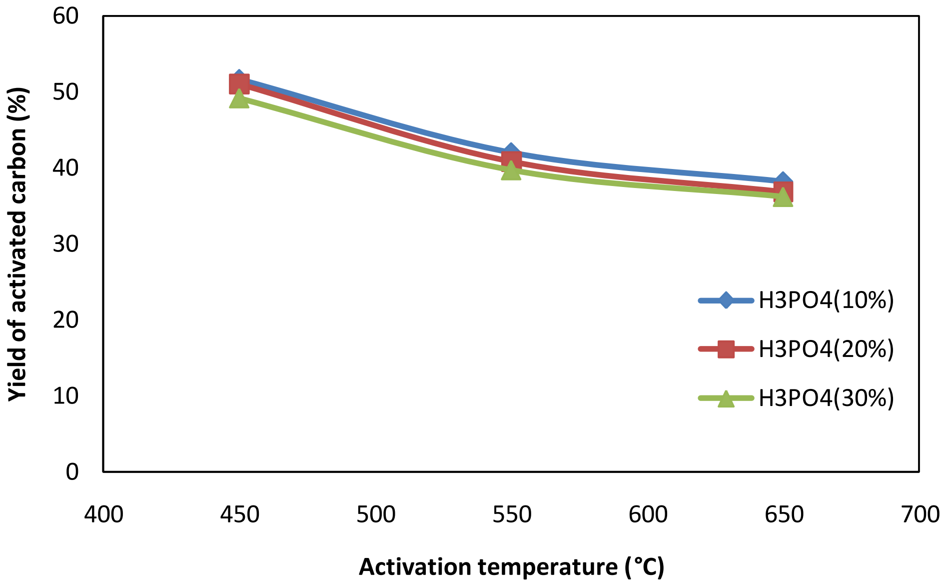

Figure 4.1. The effect of activation temperature on the yield of activated carbon (retention time: 1 h)

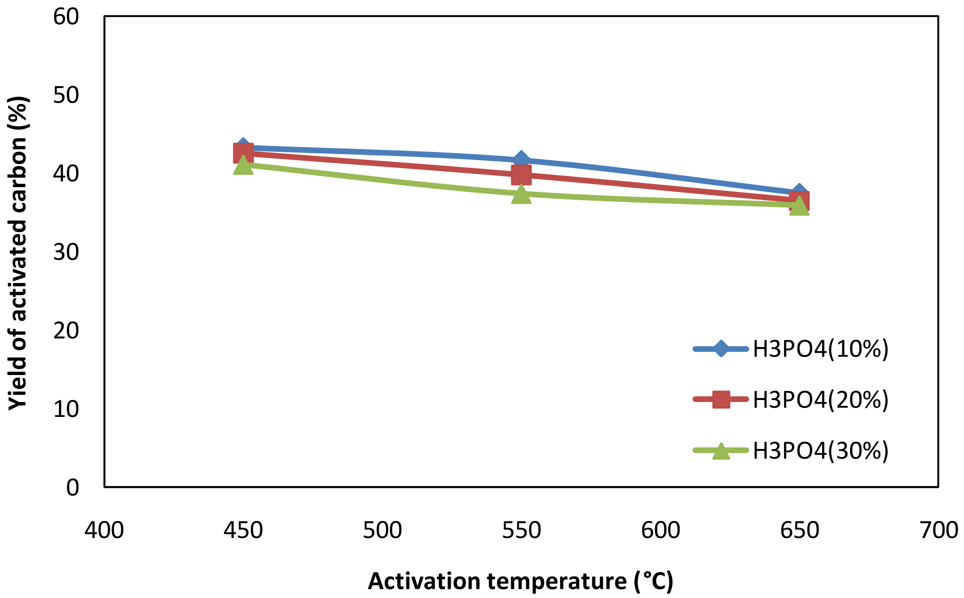

Figure 4.2. The effect of activation temperature on the yield of activated carbon (retention time: 2 h)

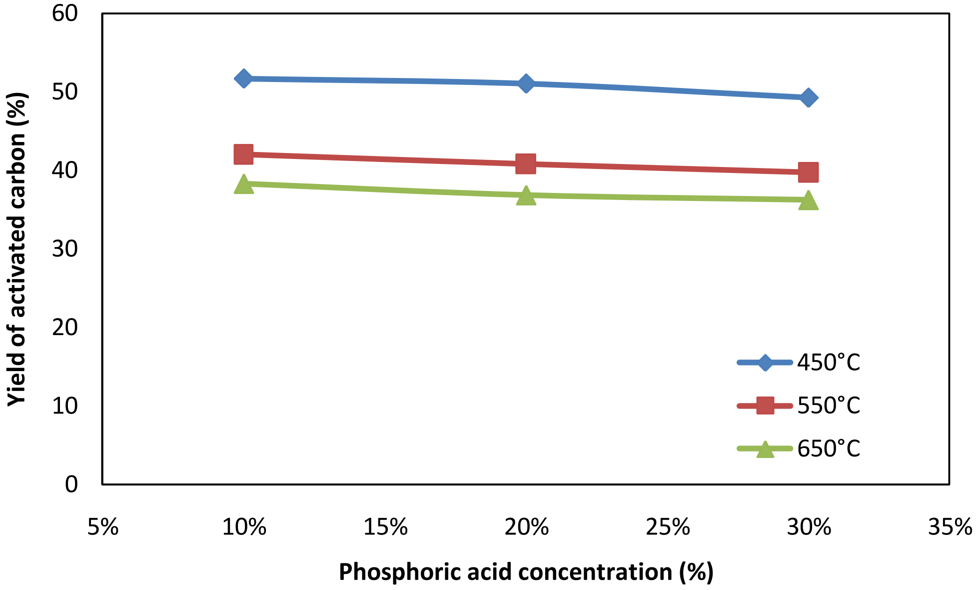

Figure 4.3. The effect of phosphoric acid on the yield of activated carbon (retention time: 1 h)

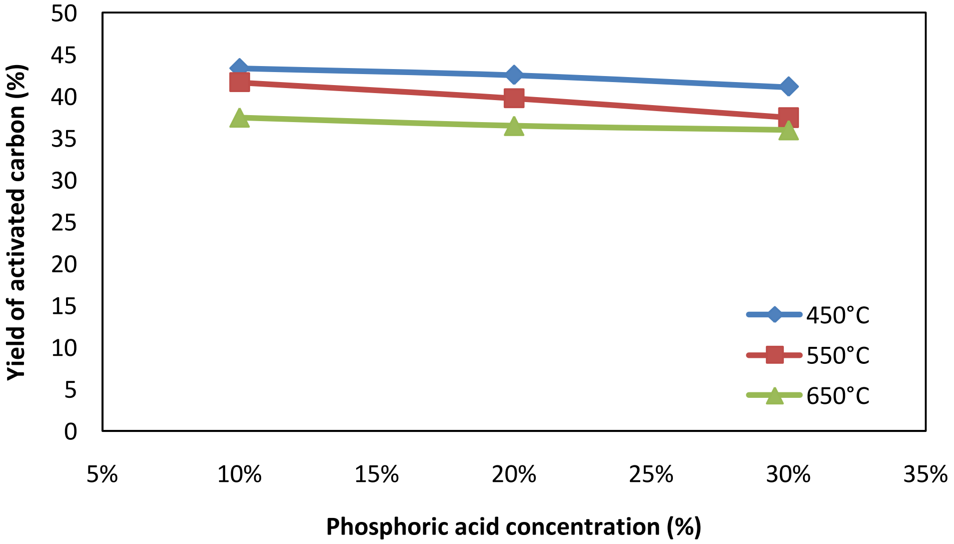

Figure 4.4. The effect of phosphoric acid on the yield of activated carbon (retention time: 2 h)

As phosphoric acid is a catalyst in the activated carbon production process, more phosphoric acid enhance the reactions of gasification, degradation and dehydration more significantly, which increases the loss of volatile and decrease the yield of final product of activated carbon.

4.3.3 Effect of retention time on yield of activated carbon from fermentation residues

The effect of retention time on the yield of activated carbon is shown in Figures 4.5, 4.6 and 4.7.

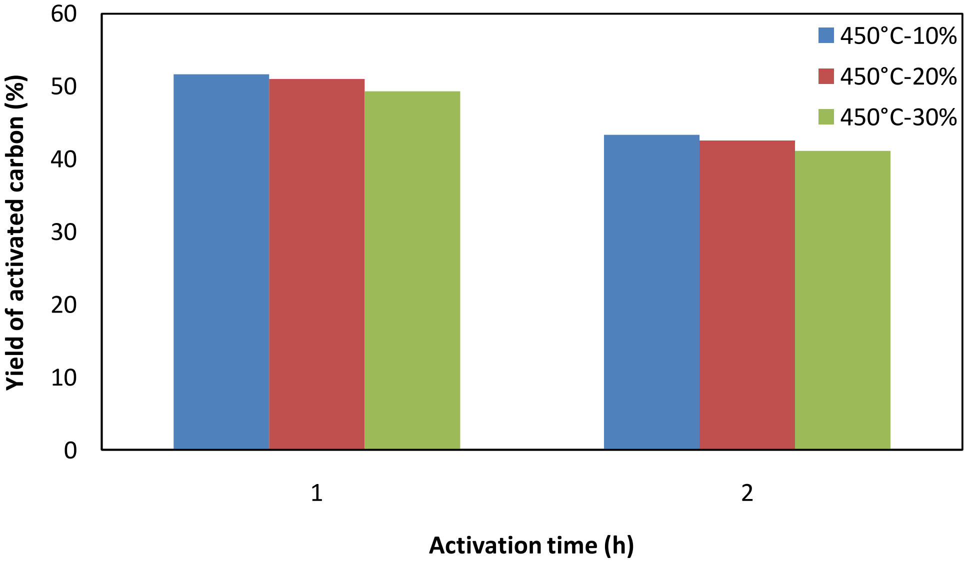

Figure 4.5. The effect of retention time on the yield of activated carbon (activation temperature: 450°C)

The yield of final product of activated carbon deceases as the retention time is increased from 1 h to 2 h because more gaseous products and volatile matters is released over longer retention time for gasification, dehydration and degradation.

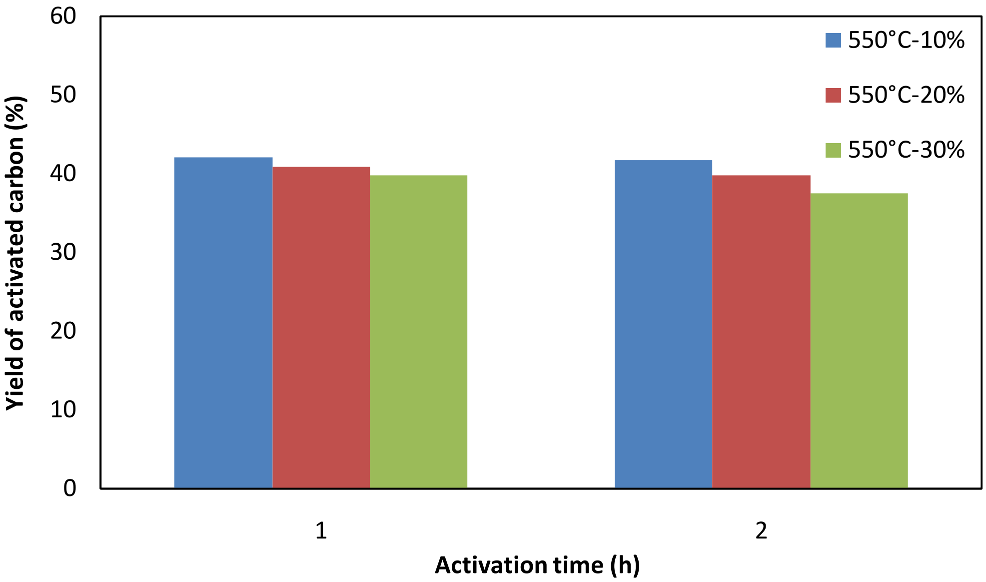

Figure 4.6. The effect of retention time on the yield of activated carbon (activation temperature: 550°C)

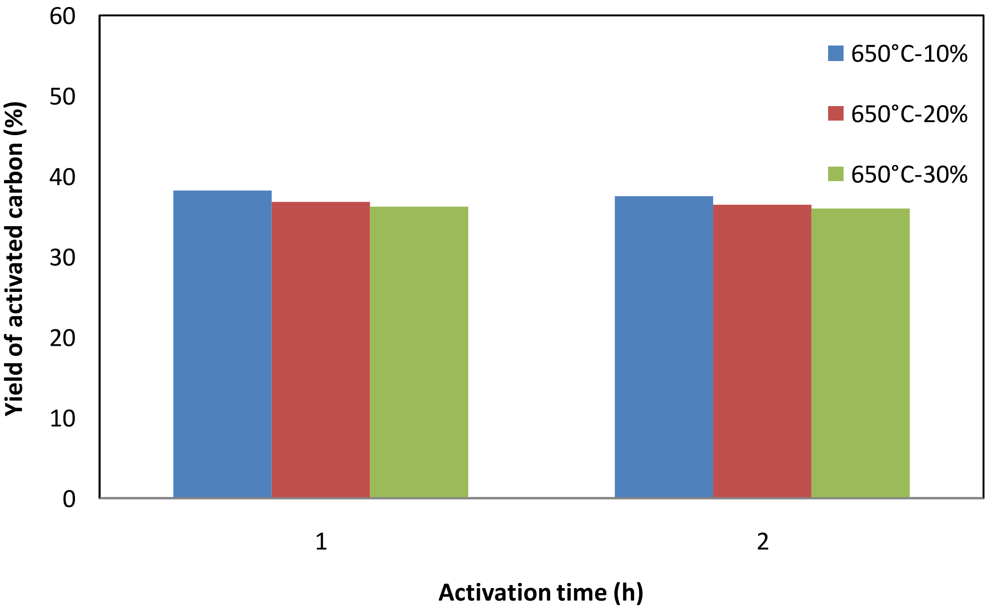

Figure 4.7. The effect of retention time on the yield of activated carbon (activation temperature: 650°C)

It can be seen from Figure 4.5 that with the increase in the retention time, the yields of activated carbons at the activation temperature of 450°C decreases more rapidly than those of the activated carbon produced at 550°C and 650°C shown Figures 4.6 and 4.7. At the activation temperatures of 550°C and 650°C, the retention time has negligible effect on the yield of activated carbon.

4.3.4 Effect of temperature on porosity development

The effect of the activation temperature on the porosity development of activated carbon produced from fermentation residues is shown in Figures 4.8 and 4.9. It is obviously seen that temperature has an adverse or detrimental effect on the porosity development of final product of activated carbon. If the activation temperature increases from 450°C to 550°C, the BET surface area decreases significantly. For the fermentation residues impregnated with 20% phosphoric acid and activated for 1 h, the BET surface area decreased by 195% from 513 m^2/g to 174 m^2/g if the activation temperature was increased from 450°C to 550°C. The BET surface area of the activated carbon was slightly decreased from 174 m^2/g to 132 m^2/g if the activation temperature was further increased from 550°C to 650°C. The decrease of the surface area with the increase of activation temperature is because more micro- and meso-pores that contribute to most of the surface area were damaged at higher activation temperatures.

Table 4.3 shows the micro-pore volumes, meso-pore volumes and total pore volumes of the activated carbons produced from fermentation residues impregnated with 20% phosphoric acid and activated for 1 h. As the activation temperature increased from 450°C to 650°C, the micro-pore volume decreased from 0.179 to 0.037 cc/g.

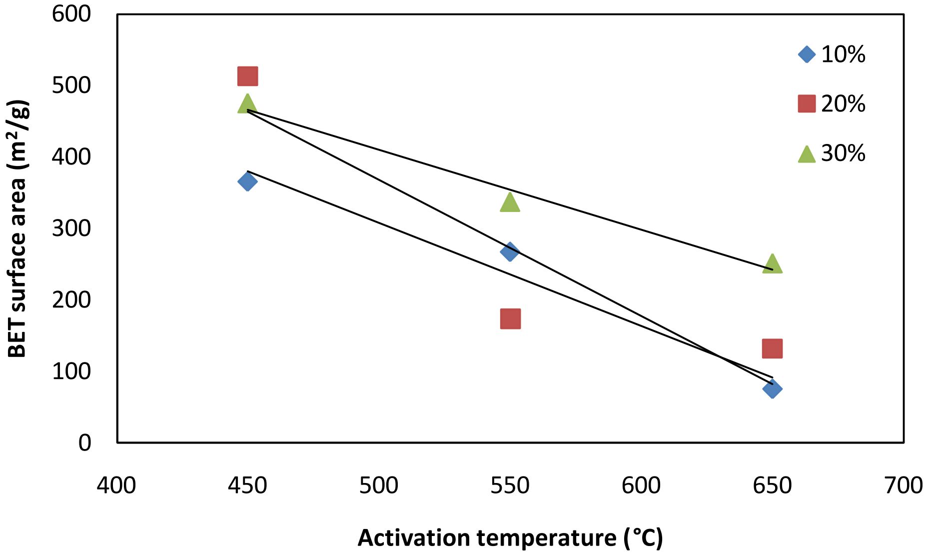

Figure 4.8. The effect of activation temperature on the porosity development (retention time: 1 h)

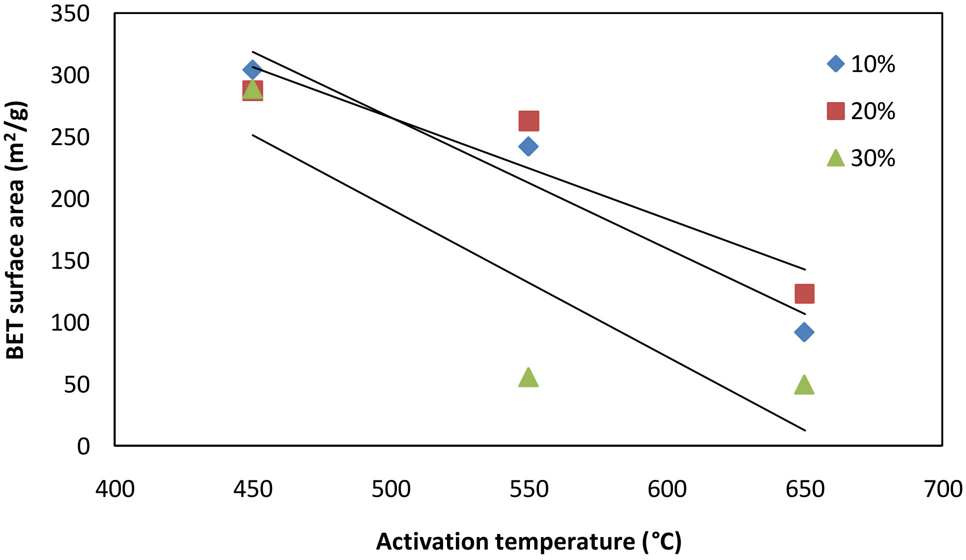

Figure 4.9. The effect of activation temperature on the porosity development (retention time: 2 h)

The number of micro-pores of activated carbon decreased greatly as temperature increased from 450°C to 650°C, because at higher temperature, more carbon might be burnt off, which damage micro-pores.

Table 4.3. Effect of temperature on pore volume of activated carbon produced from fermentation residues impregnated by 20% H_3PO_4 for 1 h

Activation temperature (°C)	**Phosphoric acid concentration (%)**	**Micro-pore volume (cc/g)**	**Meso-pore volume (cc/g)**	**Total pore volume (cc/g)**
450	20	0.179	0.123	0.302
550	20	0.063	0.071	0.134
650	20	0.037	0.066	0.103

Meso-pore volume also decreased as activation temperature increased from 450°C to 650°C. Therefore the reduction of BET surface area is caused by the burning-off micro-and meso-pores especially micro-pores. At higher temperature, the transformation of micro-pores to meso and even macro-pores is not significantly.

4.3.5 Effect of phosphoric acid concentration on porosity development

The effect of phosphoric acid concentration on the porosity development of activated carbon produced from fermentation residues is given in Figures 4.10 and 4.11. The effect of phosphoric acid with concentrations ranging from 10% to 30% on the BET surface area can be divided into three categories among different activated carbon species prepared at different temperatures and retention time. For activated carbon produced from fermentation residues impregnated with phosphoric acid and activated at an activation temperature of 450°C for 1 h, the BET surface area increased from 365 to 513 m^2/g if the phosphoric acid concentration increased from 10% to 20%. However, the surface area decreased from 513 to 476 m^2/g if the concentration of phosphoric acid was further increased from 20% to 30%.

For some samples of activated carbons, 20% phosphoric acid in the impregnation process may not the best in developing porosity and surface area of the activated carbon. For instance, BET surface area of activated carbon samples produced at 550°C for 1 h decreased from 267 to 174 m^2/g as acid concentration increased from 10% to 20% while further increased acid concentration from 20% to 30% may enhance BET surface area from 174 to 337m^2/g.

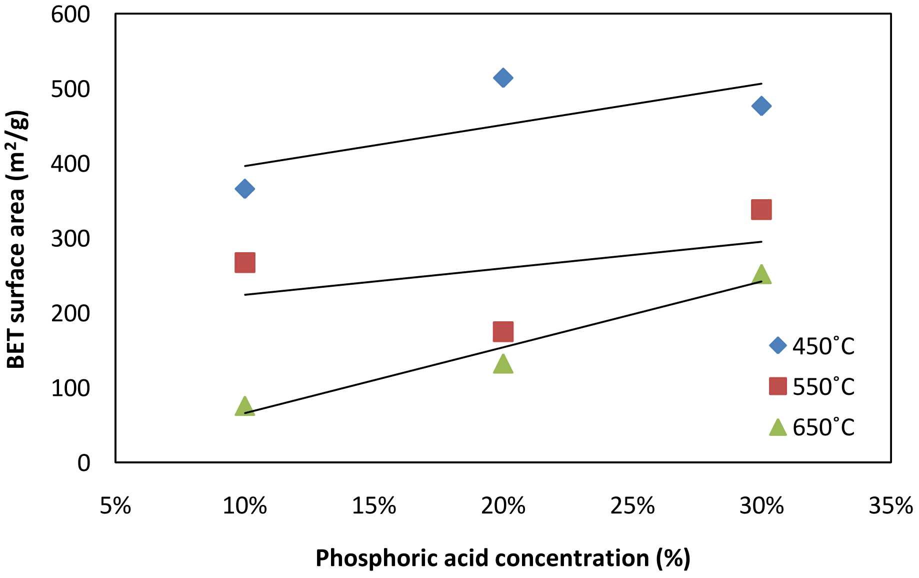

Figure 4.10. The effect of phosphoric acid on the porosity development (retention time: 1 h)

It can be observed from Table 4.4 that increased acid concentration from 10% to 20% would have an effect of transforming more micro-pores into meso-pores when precursors were activated at 550°C for 1h, resulting in the reduction of total pore volume and BET surface area.

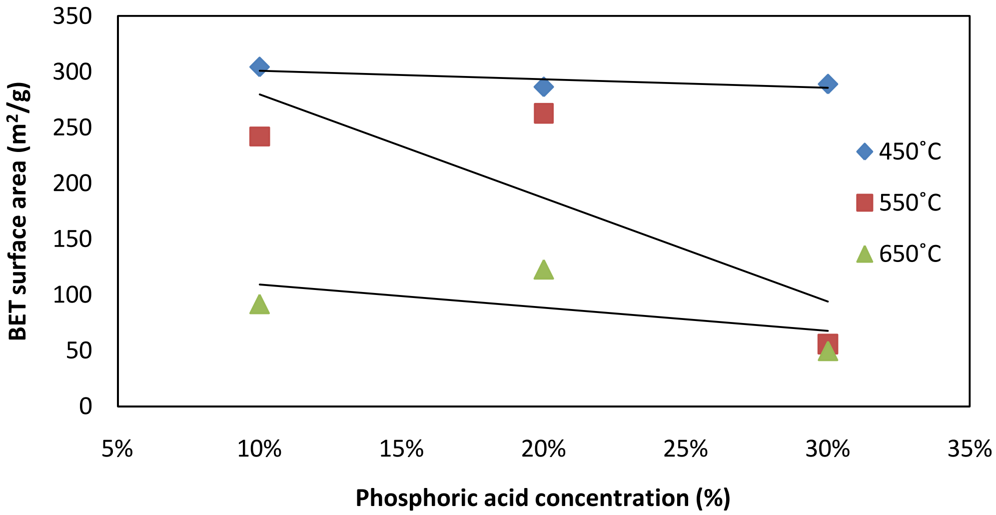

Figure 4.11. The effect of phosphoric acid on the porosity development (retention time: 2 h)

As phosphoric acid concentrations increased from 10% to 20%, the micro-pore volume increased from 0.137 to 0.179 cc/g, which could contribute to the increase in BET surface area. Meso-pore volume also increased from 0.084 to 0.123 cc/g. It can be seen from Table 5.4 that 20% phosphoric acid solution can serve as an effective catalyst in carbonization/activation process to develop micro-pores and meso-pores if the activation temperature was 450^{o}C. However, if the phosphoric acid concentration increased from 20% to 30%, more micro-pores would be developed into meso-pores, which leads to the reduction of BET surface area.

However, for certain species of activated carbon, phosphoric acid with increased concentrations would have an advantageous effect in producing more porosity and surface area. This can be illustrated by the three species of activated carbon produced at 650°C for 1h. BET surface area of final product of activated carbon increased from 75 to 251 m^2/g as raw materials of fermentation residues were impregnated with more condensed phosphoric acid. It can be seen from Table 4.4 under these processing conditions phosphoric acid with increased concentration might serve critically as a catalyst in developing micro-pores and meso-pres significantly which increased the total pore volume and BET surface area of the carbon product.

Table 4.4. Effect of phosphoric acid concentration on pore volume

Activation temperature (°C)	H_3PO_4 concentration (%)	Micro-pore volume (cc/g)	Meso-pore volume (cc/g)	Total pore volume (cc/g)
450	10	0.137	0.084	0.221
450	20	0.179	0.123	0.302
450	30	0.146	0.155	0.301
550	10	0.113	0.052	0.165
550	20	0.063	0.071	0.134
550	30	0.096	0.151	0.247
650	10	0.018	0.068	0.084
650	20	0.037	0.066	0.103
650	30	0.066	0.133	0.199

4.3.6 Effect of retention time on porosity development

The effect of retention time on the porosity development of activated carbon is shown in Figures 4.12, 4.13 and 4.14. It can be seen that the BET surface area decreased if the activation time increased from 1 h to 2 h for all samples except two samples that were (1) impregnated with 20% phosphoric acid and activated at 550^{o}C and impregnated with 10% phosphoric acid and activated at 650^{o}C. For example, for the activated carbon produced from fermentation residue impregnated with 30% phosphoric acid and activated at 550°C, the BET surface area decreased from 337 to 56 m^2/g if the activated increased from 1 h to 2 h. During activation, the burning-off of carbon structure and the transformation of micro-pores to meso-pores contribute to the decrease of the BET surface area. With the increase of activation time, more carbon was burnt off and more micro-pores were transformed to meso-pores.

As shown in Table 4.5, with the increase of activation time from 1 h to 2 h, the volumes of both micro-pores and meso-pores significantly decreased and thus the surface area decreased. Therefore, under the extremely harsh conditions (30% phosphoric acid, 550^{o}C and 2 h activation), most of micro-and meso-pores were break down due to the burning off of the carbon structure.

As shown in Table 4.6, for the activated carbon impregnated with 10% phosphoric acid and activated at 550°C, if the activation time increased from 1 h to 2 h, micro-pore volume decreased from 0.113 to 0.1 cc/g while the meso-pore volume increased from 0.052 to and 0.06 cc/g, leading to the reduction of total pore volume and BET surface area.

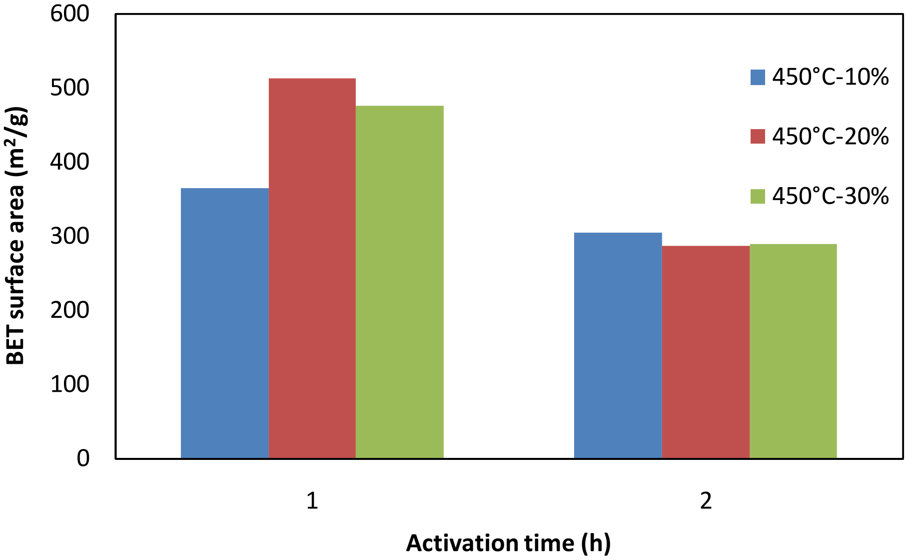

Figure 4.12. The effect of retention time on the porosity development (activation temperature: 450°C)

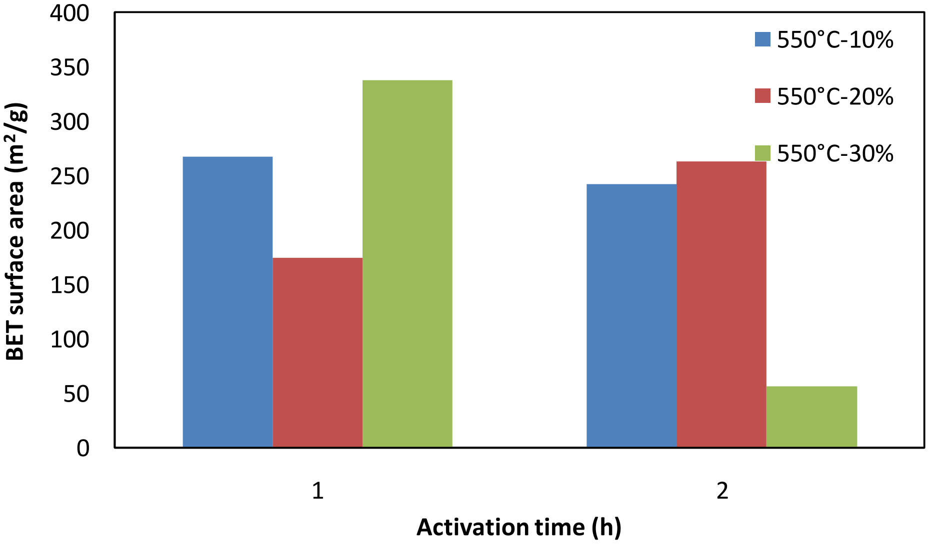

Figure 4.13. The effect of retention time on the porosity development (activation temperature: 550°C)

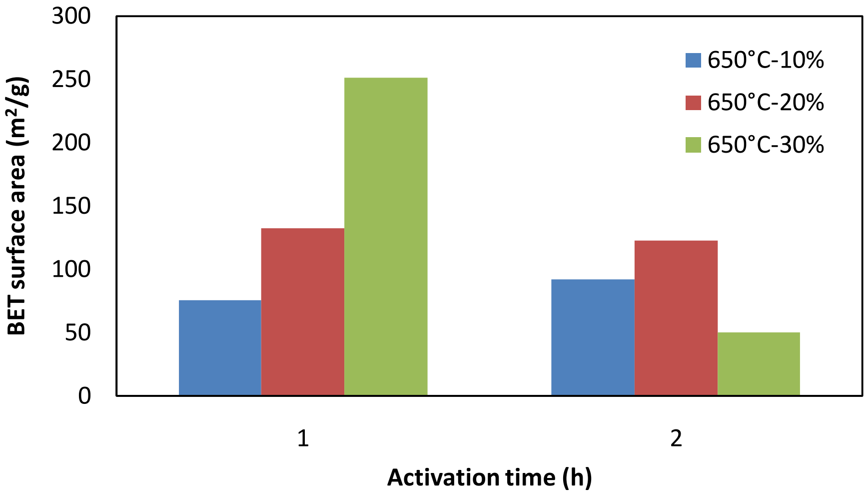

Figure 4.14. The effect of retention time on the porosity development (activation temperature: 650°C)

Table 4.5. Effect of retention time on the change of pore volume (H_3PO_4: 30%)

Activation time (h)	Activation temperature (°C)	H_3PO_4 concentration (%)	Micro-pore volume (cc/g)	Meso –pore volume (cc/g)	Total pore volume (cc/g)
1	550	30	0.096	0.151	0.247
2	550	30	0.013	0.054	0.067

Table 4.6. Effect of retention time on the change of pore volume (H_3PO_4: 10%)

Activation time (h)	Activation temperature (°C)	H_3PO_4 concentration (%)	Micro-pore volume (cc/g)	Meso -pore volume (cc/g)	Total pore volume (cc/g)
1	550	10	0.113	0.052	0.165
2	550	10	0.100	0.060	0.160

However, for two samples that were (1) impregnated with 20% phosphoric acid and activated at 550°C and impregnated with 10% phosphoric acid and activated at 650°C, the increased activation time had a positive effect on the development of porosity and the BET surface area of activated carbon. For two sample impregnated with 20% phosphoric acid and activated at 550°C, if the retention time increased from 1 h to 2 h, the total pore volume and BET surface area increased from 0.134 cc/g to 0.186 cc/g and 174 m^2/g to 263 m^2/g, respectively. As shown in Table 4.7, the increase of activation time would help to develop both micro-pores and meso-pores in the carbon product in particular for micro-pores which increased from 0.063 to 0.1 cc/g if the activation time increased from 1 h to 2 h.

Table 4.7. Effect of retention time on the change of pore volume (H_3PO_4: 20%)

Activation time (h)	Activation temperature (°C)	H_3PO_4 concentration (%)	Micro-pore volume (cc/g)	Meso - pore volume (cc/g)	Total pore volume (cc/g)
1	550	20	0.063	0.071	0.134
2	550	20	0.100	0.086	0.186

4.3.7 Optimization of activation conditions for activated carbon production from fermentation residues

The BET surface area, porosity development and yield of different species of activated carbons produced at different conditions are summarized in Table 4.8. BET surface areas are from 50-513 m^2/g while yields are from 35.96-51.68%.

Table 4.8. BET surface areas and pore volumes of activated carbons obtained at different activation conditions

Activation temperature (°C)	H_3PO_4 concentration (%)	Activation time (h)	BET surface area (m^2/g)	Micro-pore volume (cc/g)	Meso-pore volume (cc/g)	Total-pore volume (cc/g)	Yield (%)
450	10	1	365	0.137	0.084	0.221	51.68
450	20	1	513	0.179	0.123	0.302	51.04
450	30	1	476	0.146	0.155	0.301	49.24
550	10	1	267	0.113	0.052	0.165	42.08
550	20	1	174	0.063	0.071	0.134	40.84
550	30	1	337	0.096	0.151	0.247	39.76
650	10	1	75	0.018	0.066	0.084	38.28
650	20	1	132	0.037	0.066	0.103	36.84
650	30	1	252	0.066	0.133	0.199	36.24
450	10	2	304	0.116	0.093	0.209	43.32
450	20	2	286	0.102	0.089	0.191	42.52
450	30	2	289	0.098	0.114	0.212	41.12
550	10	2	242	0.100	0.060	0.160	41.68
550	20	2	263	0.100	0.086	0.186	39.76
550	30	2	56	0.013	0.054	0.067	37.44
650	10	2	92	0.031	0.058	0.089	37.48
650	20	2	123	0.041	0.086	0.127	36.48
650	30	2	50	0.011	0.048	0.059	35.96

It is obviously seen that fermentation residues impregnated with 20% phosphoric acid followed by activation at 450°C for 1 h can produce activated carbon for which the BET surface area is over 500 m^2/g and the total pore volume is 0.302 cc/g.

The effect of different production conditions including activation temperature, phosphoric acid concentration and retention time was already discussed earlier in the above sections.

The liquid nitrogen adsorption isotherm and desorption isotherm of activated carbon prepared at optimized conditions are displayed in Figure 4.15.

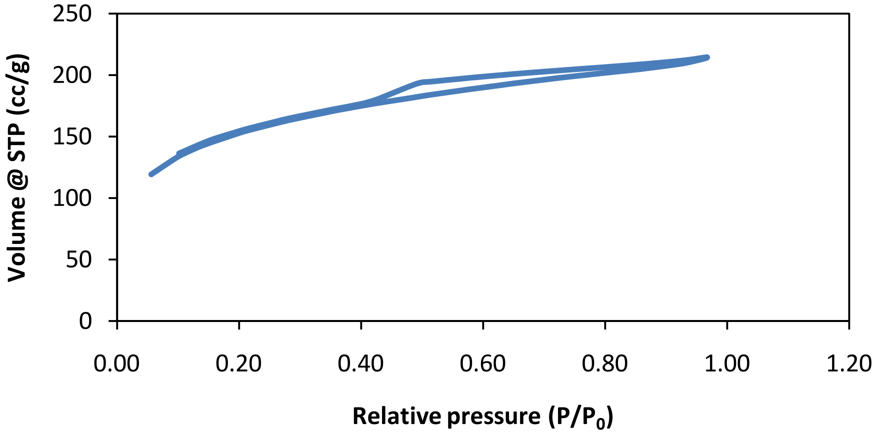

Figure 4.15. Liquid nitrogen adsorption isothermal and desorption isothermal of activated carbon prepared from fermentation residues under the optimized conditions

Figure 4.16 and Figure 4.17 show the pore size distribution of the species of activated carbon produced at the optimized process conditions in which fermentation residues were impregnated by 20% phosphoric acid followed by carbonization/activation at 450°C for 1 h. It is observed in Fig and Fig that as the half pore size increases from approximately 0.8 to 2.5 nm, the cumulative pore volume and BET surface area increase strikingly; however, after pore size increases from 2.5 to 10 nm, the improvement of cumulative pore volume and BET surface area increase very slowly.

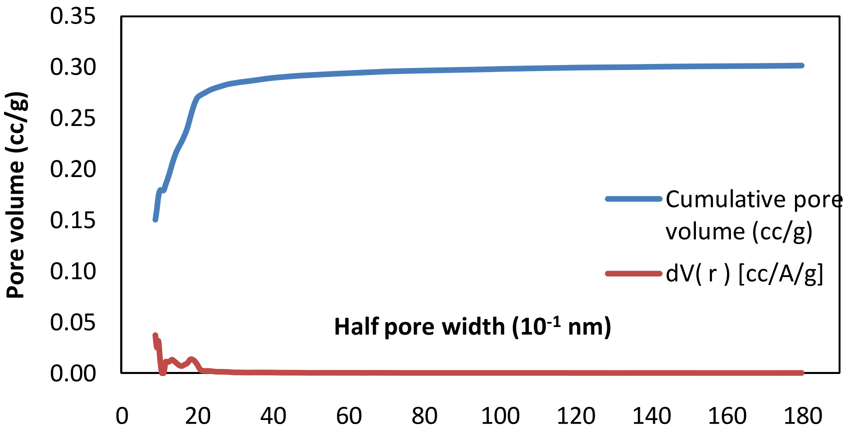

Figure 4.16. Pore size distribution of activated carbon prepared from fermentation residues under the optimized conditions

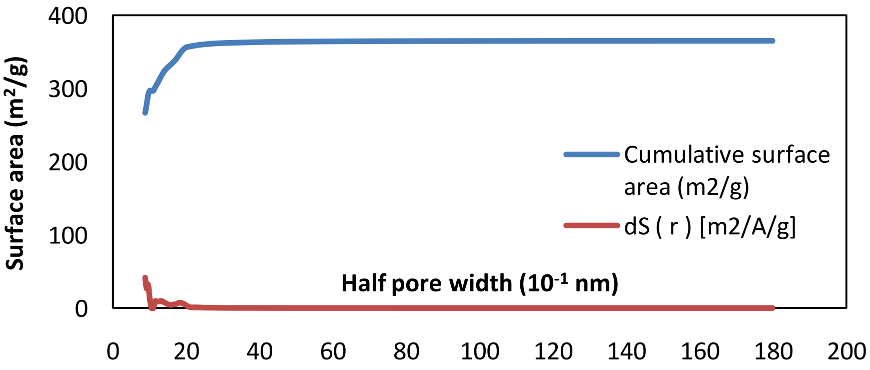

Figure 4.17. BET surface area distribution of activated carbon prepared from fermentation residues under the optimized conditions

It is also seen those pores of size larger than 10 nm can hardly contribute to the development of cumulative pore volume and BET surface area.

From Table 4.9, it can be seen micro-pore surface area and micro-pore volume of the species of activated carbon produced at the optimized conditions contribute 58% and 59% respectively to the total pore volume and BET surface area. Moreover, it can be observed from Figure 5.16 and Figure 5.17 there are three peaks of pores at approximately 1 nm, 1.25 nm and 1.75 nm.

Table 4.9. Pore volume of activated carbon from fermentation residues at the optimized conditions

Property	Micro-pore	Meso-pore	Total-pore
Pore volume (cc /g)	0.179	0.123	0.302
BET surface area (m^2/g)	297	216	513

4.3.8 Thermal gravimetric analysis (TGA) of impregnated fermentation residues

Weight loss of fermentation residues impregnated by phosphoric acid of different concentrations is shown in Figure 4.18, Figure 4.19 and Figure 4.20. It is observed that the two large weight loss rates happened around 60-70°C and 200-230°C. The dramatically increased weight loss rate around 60-70°C is due to the loss of water and the dramatically increased weight loss rate around 200-230°C is due to the evaporation of phosphoric acid.

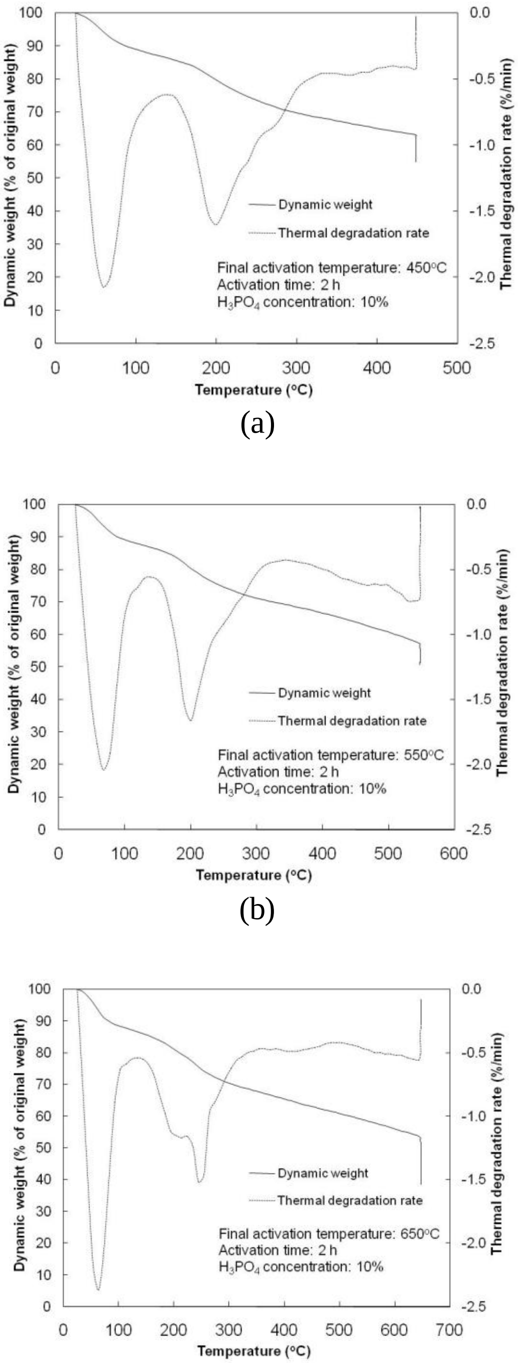

(a)

(b)

(c)

Figure 4.18. (a) (b) (c) Thermal gravimetric analysis of thermal degradation of fermentation residues impregnated with 10% H_3PO_4 during activation in nitrogen.

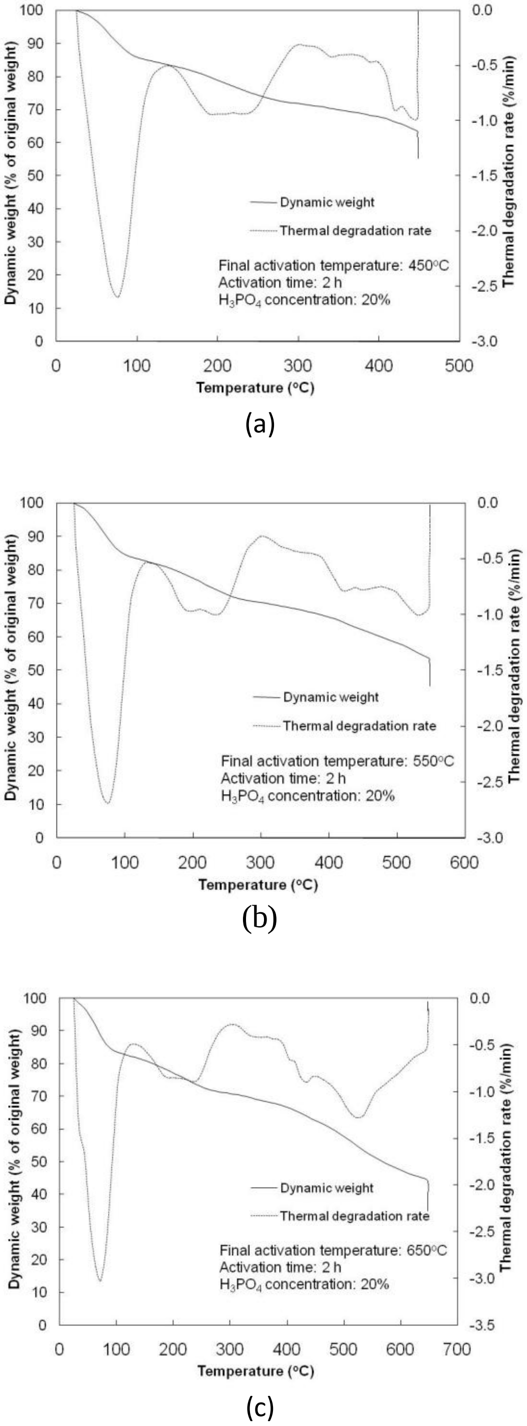

Figure 4.19. (a) (b) (c) Thermal gravimetric analysis of thermal degradation of fermentation residues impregnated with 20% H_3PO_4 during activation in nitrogen.

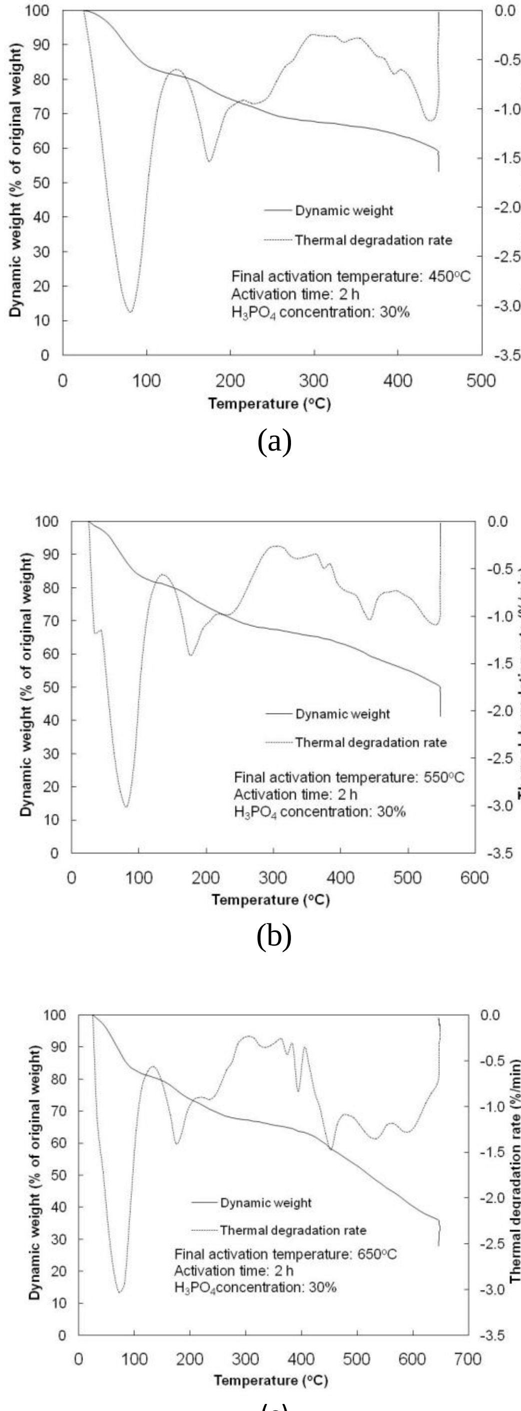

(a)

(b)

(c)

Figure 4.20. (a) (b) (c) Thermal gravimetric analysis of thermal degradation of fermentation residues impregnated with 30% H_3PO_4 during activation in nitrogen.

4.4 Comparison of Activated Carbon Prepared from Fermentation Residues and Agricultural Residues

Table 4.10 gives the comparison of the porosity development of activated carbon produced from fermentation residues and raw agricultural residues. From Table 4.10, it can be seen that the BET surface area of activated carbon prepared from switch grass-derived fermentation residue impregnated by phosphoric acid at 20% concentration and activated at 450^{o}C for 1 h can reach up to 513m^2/g while the BET surface area of activated carbon prepared from raw switch grass at the same conditions is only 211 m^2/g.

Table 4.10. Comparison of activated carbon from fermentation residues and agricultural residues impregnated by 20% H_3PO_4 and activated at 450°C for 1 h

Raw material of activated carbon	BET surface area (m^2/g)	Micro-pore volume (cc/g)	Meso-pore volume (cc/g)	Total-pore volume (cc/g)
Switch grass fermentation residue	513	0.179	0.123	0.302
Switch grass 1mm	211	0.089	0.056	0.145
Switch grass 2mm	96	0.034	0.051	0.085

Information from various literature shows that the optimal activation temperature for producing high quality activated carbon from various raw materials is below 500°C [12, 46, 84-86]. However, the optimized retention time in literature is usually more than 1 h [12, 46, 84-86] instead of 1 h which is optimal in producing activated carbon from fermentation residues. Moreover, in most of the research on activated carbon production by phosphoric acid activation, the optimized concentration of phosphoric acid is usually higher than 50% or even as high as 85% [12, 46, 84-86].

Higher surface area of activated carbon produced from fermentation residues using lower retention time and phosphoric acid at lower concentration might be because the pretreatment of raw material before fermentation process favored the porosity development during the activation process. Nevertheless, further research is needed to investigate the correlation of pretreatment of raw material before fermentation residues and the porosity development of carbon product during the activation process.

4.5 Production of Activated Carbon from Pyrolysis Residues

4.5.1 Yield of activated carbon prepared from pyrolysis residues

Table 4.11 gives the yield of activated carbon produced from pyrolysis residues. It can been seen that the activated carbons prepared from the pyrolysis residues have higher yield than those prepared from the fermentation residues because more than 65% of raw materials have already lost during the pyrolysis process at 450°C for 1 h. As most of the volatile matters were released during the pyrolysis (carbonization) process, the carbon content of pyrolysis residues is significantly enriched, ranging from 54 to72%.

4.5.2 Characterization of porosity development of pyrolysis residues

Table 4.12 shows that the pyrolysis residues or biochars from different pyrolysis process have a surface area from 20 to 79 m^2/g, which are generated by the release of volatile matters and gaseous products in the biomass during pyrolysis or carbonization. However, the surface areas of these pyrolysis residues are very low compared to that of activated carbon because only carbonization happened to develop some rudimentary pores during pyrolysis while the activation with oxidizing gas or chemicals is needed to develop large numbers of micro-pores in activated carbon.

Table 4.11. Yield of activated carbon prepared from pyrolysis residues

Biomass	Yield of activated carbon (%)	Weight loss during pyrolysis (%)	C content of pyrolysis residue (%)
Wheat straw	51.15	67.5	72.2
Switch grass	53.52	69.0	54.0
Corn stover	54.13	67.8	54.9

Table 4.12. Porosity development of residues from pyrolysis process

Biomass	BET surface area (m^2/g)	Micro-pore volume (cc/g)	Meso-pore volume (cc/g)	Total pore volume (cc/g)
Wheat straw	79.189	0.069	0.031	0.100
Switch grass	45.769	0.038	0.030	0.068
Corn stover	20.529	0.025	0.015	0.040

4.5.3 Characterization of porosity development of activated carbon from pyrolysis residues

Table 4.13 gives the he porosity development of activated carbons produced from pyrolysis residues. It can be seen that the activated carbons prepared from pyrolysis residues impregnated with KOH and activated at a high temperature of 780°C have large surface areas of 957, 874 and 971 m^2/g for the wheat straw, switch grass, and corn stover derived biochars, respectively. The total pore volume of the activated carbons produced from wheat straw, switch grass and corn stover derived biochars were 0.525, 0.491 and 0.531 cc/g, respectively.

Compared to activated carbon prepared by fermentation residues impregnated with H_3PO_4, activated carbon prepared from pyrolysis residues impregnated with KOH has a much better porosity development, because of the rudimentary porosity of the pyrolyisis residues generated during pyrolysis and the severe reaction between carbon and KOH at a high temperature during activation, which produces hydrogen to further develop porosity on those existing rudimentary porosity sites.

Table 4.13. Porosity development of activated carbons produced from pyrolysis residues

Biomass	BET surface area (m^2/g)	Total pore volume (cc/g)
Wheat straw	1147	0.639
Switch grass	874	0.491
Corn stover	971	0.531

4.6 Catalyst Development

4.6.1 Characterization of Fe catalyst supported on activated carbon prepared from fermentation and pyrolysis residues

The surface area, micro-pore volume and total pore volume of activated carbon produced from fermentation residues at optimized conditions (AC-FR), activated carbon produced from pyrolysis residues of wheat straw (AC-PR), and catalysts developed on these two activated carbons are given in Table 4.14.

It can be seen that the BET surface area and total pore volume of Fe-catalyst on AC-FR decreased from 513 m^2/g for the AC-FR to 359 m^2/g and 0.302 cc/g for the AC-FR to 0.214 cc/g, respectively. On the other hand, it can be found that the BET surface area and total pore volume of Fe-catalyst on AC-PR decreased from 1147 m^2/g for the AC-PR to 488 m^2/g, and 0.639 cc/g for the AC-PR to 0.268 cc/g, respectively.

Table 4.14. Comparison of BET surface areas and pore volumes of activated carbons from fermentation and pyrolysis residues and Fe catalyst supported on them

	BET surface area (m^2/g)	**Micro-pore volume (cc/g)**	**Total pore volume (cc/g)**
AC-FR	513	0.179	0.302
Fe-catalyst (AC-FR)	359	0.111	0.214
AC-PR	1147	0.476	0.639
Fe-catalyst (AC-PR)	488	0.199	0.268

The BET surface area and total pore volume of Fe-catalyst on the AC-FR decreased by 30% and 29% respectively compared to the decreases by 57% and 58% for that of Fe-catalyst on the AC-PR. The reason that the AC-PR has a much stronger adsorption capacity is because the BET surface area and pore volume of AC-PR are much larger than those of AC-FR. Meantime, AC-PR has more micro-pores which favor adsorbing more small molecules like $Fe(NO_3)_3 \cdot H_2O$.

4.6.2 Weight loss analysis of catalysts developed on activated carbon produced from fermentation and pyrolysis residues

Weight loss of catalysts developed on activated carbon produced from fermentation and pyrolysis residues is shown in Figure 4.21. It is observed that the weights of the catalysts developed on activated carbons from fermentation and pyrolysis residues decreased to 88.74% and 92.04% of their original weight. The weight loss of catalyst developed on activated carbon from fermentation residues is more, because activation temperature of pyrolysis residues is much higher which has already released more volatile matters and gaseous products.

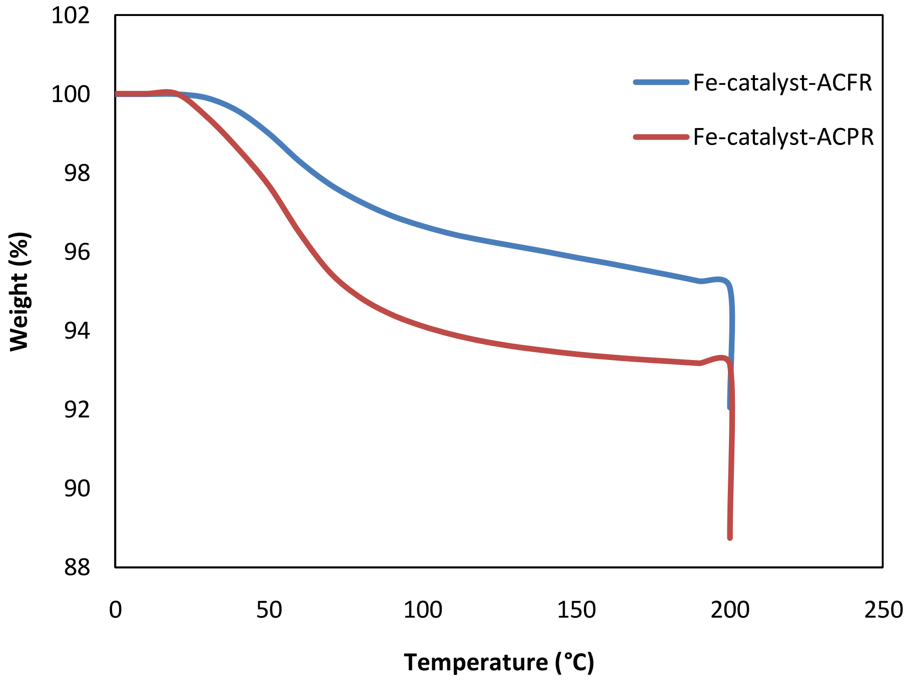

Figure 4.21. Weight loss of catalysts developed on activated carbon from fermentation and pyrolysis residues

4. 7 Statistical Analysis

4.7.1 Replicates of experiments

Selected replicates of experiments of activated carbon produced from fermentation residues are given in Table 4.15 and Table 4.16. It can be seen that different results of replicates are compatible with each other and the relative standard deviation is lower than the upper limit of the acceptable range of 5%.

Table 4.15. Replicates of activated carbon produced from fermentation residues impregnated by 20% H_3PO_4 and activated at 550°C for 1 h

	Replicate 1	**Replicate 2**	**Average**	**Standard deviation**	**Relative standard deviation (%)**
BET surface area (m^2/g)	166	174	170	5.65	3.32
Total pore volume (cc/g)	0.133	0.134	0.1335	0.0007	0.53
Yield (%)	40.84	41.55	41.20	0.50	1.21

Table 4.16. Replicates of activated carbon produced from fermentation residues impregnated by 10% H_3PO_4 and activated at 550°C for 2 h

	Replicate 1	**Replicate 2**	**Average**	**Standard deviation**	**Relative standard deviation (%)**
BET surface area (m^2/g)	242	239	240.5	2.12	0.88
Total pore volume (cc/g)	0.160	0.159	0.1595	0.0007	0.44
Yield (%)	41.68	42.35	42.02	0.47	1.12

4.7.2 Regression analysis

4.7.2.1 Linear regression model

A 3×3×2 factorial design was used to analyze the process for producing activated carbon from fermentation residues. The results from 18 tests with all combinations of x_1, x_2 and x_3, and the BET surface area Y_1, total pore volume Y_2 and yield Y_3 of each test were given in Table 4.8.

The linear regression model that was used to fit the experimental data in Table 4.8 is:

$$Y = a_0 + a_1x_1 + a_2x_2 + a_3x_3 + a_{12}x_1x_2 + a_{13}x_1x_3 + a_{23}x_2x_3 + a_{123}x_1x_2x_3$$

where Y is the response variables of the yield, BET surface area and total pore volume of activated carbon; x_1,x_2,x_3 are process variables of activation temperature, activation time and acid concentration; a_0, a_1, a_2, a_3, a_{12}, a_{13}, a_{23}, a_{123} are the coefficients determined by regressing the experimental data. Regression analysis of the experimental data was done using the Microsoft Excel. Statistical parameters of various models are given in Table 4.17, Table 4.18, Table 4.19, Table 4.20, Table 4.21 and Table 4.22.

The following regression models can be used to predict the BET surface area, pore volume and yield of activated carbon produced from fermentation residues at a specific condition:

$$Y_1 = 1581.92 - 2.76x_1 - 5.88x_2 - 411.44x_3 + 0.04x_1x_2 + 0.93x_1x_3 + 2.77x_2x_3 - 0.02$$

$$Y_2 = 0.7984 - 0.0014x_1 - 0.0029x_2 - 0.1979x_3 + 0.0005x_1x_3 + 0.0027x_2x_3$$

$$Y_3 = 128.15 - 0.14x_1 - 1.68x_2 - 34.24x_3 + 0.05x_1x_3 + 0.72x_2x_3$$

Table 4.17. ANOVA for the regression model for the BET surface area

	df	SS	MS	F
Regression	7	272421.1	38917.3	9.3
Residual	10	41618.8	4161.8	
Total	17	314040		

Table 4.18. Results of regression analysis for the BET surface area

	Coefficient	S.E	t-value
a_0	1581.917	866.362	1.825
a_1	-2.755	1.558	-1.768
a_2	-5.879	40.104	-0.146
a_3	-411.444	547.936	-0.750
a_{12}	0.039	0.072	0.551
a_{13}	0.933	0.985	0.947
a_{23}	2.770	25.364	0.109
a_{123}	-0.023	0.045	-0.509

Table 4.19. ANOVA for the regression model for the total pore volume

	df	SS	MS	F
Regression	7	0.078221	0.011174	7.780385
Residual	10	0.014362	0.001436	
Total	17	0.092583		

Table 4.20. Results of regression analysis for the total pore volume

	Coefficient	S.E	t-value
a_0	0.798444	0.508940	1.568839
a_1	-0.001410	0.000915	-1.544100
a_2	-0.002930	0.023559	-0.124330
a_3	-0.197920	0.321882	-0.614870
a_{12}	0.000025	0.000042	0.607730
a_{13}	0.000508	0.000579	0.878109
a_{23}	0.002733	0.014900	0.183442
a_{123}	-0.000017	0.000026	-0.634380

Table 4.21. ANOVA for the regression model for the yield

	df	SS	MS	F
Regression	7	335.546	47.935	24.086
Residual	10	19.901	1.990	
Total	17	355.447		

The statistical significance of the regression model was evaluated by the F-test analysis of variance (ANOVA) which showed the regression is statistically significant at 95% of confidence level.

Table 4.22. Results of regression analysis for the yield

	Coefficient	S.E	t-value
a_0	128.1567	18.9450	6.7646
a_1	-0.1414	0.0340	-4.1500
a_2	-1.6768	0.8769	-1.9120
a_3	-34.2422	11.9818	-2.8578
a_{12}	0.0025	0.0015	1.6294
a_{13}	0.0548	0.0215	2.5430
a_{23}	0.7253	0.5546	1.3077
a_{123}	-0.0012	0.0009	-1.2029

4.7.2.2 Application of linear regression model

The BET surface area, micro-pore volume, total pore volume and yield of activated produced from fermentation residues at specific conditions can be calculated using Equations 4.2, 4.3 and 4.4. Examples of application of linear regression models are shown in Table 4.23.

Table 4.23. Application of linear regression model

Activation temperature, x_1 (°C)	H_3PO_4 concentration, x_2 (%)	Activation time, x_3 (h)	BET surface area (m^2/g)	Total pore volume (cc/g)	Yield (%)
620	12	1.2	336	0.26	49.6
530	18	1.8	631	0.46	61.7

4.8 Economic Analysis

The prices of basic equipment needed for the facilities to produce activated carbon from fermentation and pyrolysis residues are given in Table 4.24. Scaled costs of equipments for facilities to produce activated carbons from fermentation and pyrolysis residues were shown in Table 4.25 and Table 4.26.

Table 4.24. Capital costs of equipment in the facilities for producing activated carbon from fermentation and pyrolysis residues

Equipment	Processing capability (kg/d)	Cost of baseline equipment (US$)
Rotary dryer	4,000	150,000
Rotary kiln	4,000	205,000
Washing tank	4,000	80,000
Acid/base recovery tank	4,000	83,000
Acid/base storage tank	4,000	70,000
Acid/base soaking tank	4,000	80,000

Total capital costs and operating costs of the facility for producing activated carbon from fermentation and pyrolysis residues are shown in Table 4.27, Table 4.28, Table 4.29 and Table 4.30. It can be seen from Figure 4.22 and 4.23 that as the daily processing capability of a facility increases from 3000 to 9000 kg/day, the production cost of activated carbon decreases slowly as a result of economy of production scale.

Table 4.25. Scaled costs of equipment in the facilities for producing activated carbon from fermentation residues

Equipment (US$)	**Daily processing capability (kg/day)**					
	2,000	**3,000**	**4,000**	**5,000**	**6,000**	**7,000**
Rotary dryer	98,963	126,220	150,000	171,489	191,313	209,852
Rotary kiln	135,250	172,501	205,000	234,369	261,462	286,798
Washing tank	52,780	67,317	800,00	91,461	102,034	111,921
Recovery tank	54,760	69,842	830,00	94,891	105,860	116,118
Storage tank	46,182	58,903	70,000	80,028	89,280	97,931
Soaking tank	52,780	67,317	80,000	91,461	102,034	111,921
Total	638,642	814,539	968,000	1,106,678	1,234,611	1,354,248

Table 4.26. Scaled costs of equipment in the facilities for producing activated carbon from pyrolysis residues

Equipment (US$)	**Daily processing capability (kg/day)**					
	2,000	**3,000**	**4,000**	**5,000**	**6,000**	**7,000**
Rotary dryer	98,963	126,220	150,000	171,489	191,313	209,852
Rotary kiln	135,250	172,501	205,000	234,369	261,462	286,798
Washing tank	52,780	67,317	80,000	91,461	102,034	111,921
Recovery tank	54,760	69,842	83,000	94,891	105,860	116,118
Storage tank	46,182	58,903	70,000	80,028	89,280	97,931
Soaking tank	52,780	67,317	80,000	91,461	102,034	111,921
Total	539,679	688,320	818,000	935,189	1,043,297	1,144,395

Table 4.27. Capital costs of the facility for producing activated carbon from fermentation residues

Production scale (kg/day)		**3,000**	**5,000**	**7,000**	**9,000**
Direct project expenses (US$)					
Equipment	C_P	814,539	1,106,678	1,354,248	1,574,653
Materials for installation	C_M = MMF x C_P	219,925	298,803	365,647	425,156
Direct labor	C_L = LMF x (Cp + C_M)	279,305	379,480	464,372	539,948
Total direct	$C_D = C_P + C_M + C_L$	1,313,770	1,784,961	2,184,267	2,539,758
Indirect project expenses (US$)					
Freight, insurance, taxes	$C_{FIT} = 0.08C_P$	65,163	88,534	108,340	125,972
Construction overhead	$C_O = 0.7C_L$	195,514	265,636	325,060	377,964
Engineering expenses	$C_E = 0.15 (C_P + C_M)$	155,170	210,822	257,984	299,971
Total indirect	$C_{ID} = C_{FIT} + C_O + C_E$	415,847	564,992	691,384	803,908
Bare module cost	$C_{BM} = C_D + C_{ID}$	1,729,617	2,349,953	2,875,651	3,343,665
Contingency & fee	$C_{CF} = 0.18C_{BM}$	311,331	422,992	517,617	601,860
Total module cost	$C_{TM} = C_{BM} + C_{CF}$	2,040,948	2,772,945	3,393,268	3,945,525
Auxiliary facilities	$C_{AF} = 0.3C_{TM}$	612,284	831,884	1,017,980	1,183,658
Total capital	$T = C_{TM} + C_{AF}$	2,653,232	3,604,828	4,411,248	5,129,183

Table 4.28. Operating costs of the facility for producing activated carbon from fermentation residues

Production scale (kg/day)		3,000	5,000	7,000	9,000
Fermentation residues	US$ 0/kg	0	0	0	0
H_3PO_4	US$ 1/kg	168,000	280,000	392,000	504,000
Utilities	$0.129/(kg d)	136,125	226,875	317,625	408,375
Operating labor	3 shifts/d at 20$/h	336,000	672,000	1,008,000	1,344,000
Supervisory labor	15% of operating labor	50,400	100,,800	151,200	201,600
Maintenance & repairs	5% of total capital	132,662	180,241	220,562	256,459
Supplies	15% of Maintenance & repairs	19,899	27,036	33,084	38,469
Taxes	1% of total capital	26,532	36,048	44,112	51,292
Insurance	0.5% of total capital	13,266	18,024	22,056	25,646
General expenses	15% of operating labor	50,400	100,800	151,200	201,600
Annual capital charges	$C_{total}\ i\ (1+i)^n/[(1+n)^n - 1]$	348,837	473,949	579,974	674,366
Anual operating cost	Sum of the items above	1,282,121	2,115,774	2,919,815	3,705,806
Production cost ($/kg)	Annual operating cost divided by annual production output	2.44	2.41	2.38	2.35

Table 4.29. Capital costs of the facility to produce activated carbon from pyrolysis residues

Production scale (kg/day)		3,000	5,000	7,000	9,000
Direct project expenses (US$)					
Equipment	C_P	688,320	935,189	1,144,395	1,330,647
Materials for installation	$C_M = MMF \text{ x } C_P$	185,846	252,501	308,987	359,275
Direct labor	$C_L = LMF \text{ x } (Cp + C_M)$	236,025	320,676	392,413	456,279
Total direct	$C_D = C_P + C_M + C_L$	1,110,191	1,508,366	1,845,795	2,146,201
Indirect project expenses (US$)					
Freight, insurance, taxes	$C_{FIT} = 0.08C_P$	55,066	74,815	91,552	106,452
Construction overhead	$C_O = 0.7C_L$	165,217	224,473	274,689	319,395
Engineering expenses	$C_E = 0.15 (C_P + C_M)$	131,125	178,154	218,007	253,488
Total indirect	$C_{ID} = C_{FIT} + C_O + C_E$	351,408	477,442	584,248	679,335
Bare module cost	$C_{BM} = C_D + C_{ID}$	1,461,599	1,985,808	2,430,043	2,825,536
Contingency & fee	$C_{CF} = 0.18C_{BM}$	263,088	357,446	437,408	508,596
Total module cost	$C_{TM} = C_{BM} + C_{CF}$	1,724,687	2,343,254	2,867450	3,334,132
Auxiliary facilities	$C_{AF} = 0.3C_{TM}$	517,406	702,976	860,235	1,000,240
Total capital	$T = C_{TM} + C_{AF}$	2,242,093	3,046,230	3,727,685	4,334,372

Table 4.30. Production costs of the facility to produce activated carbon from pyrolysis residues

Item	Calculation	3,000	5,000	7,000	9,000
Pyrolysis residues	$114 /kg	119,700	199,500	279,300	359,100
KOH	$2.5/kg	393,750	656,250	918,750	1,181,250
Utilities	$0.149/(kg d)	157,200	262,000	366,800	471,600
Operating labor	3 shifts/d at US$ 20/h	336,000	672,000	1,008,000	1,344,000
Supervisory labor	15% of operating labor	50,400	100,800	151,200	201,600
Maintenance & repairs	5% of total capital	112,105	152,312	186,384	216,719
Supplies	15% of Maintenance & repairs	16,816	22,847	27,958	32,508
Taxes	1% of total capital	22,421	30,462	37,277	43,344
Insurance	0.5% of total capital	11,210	15,231	18,638	21,672
General expenses	15% of operating labor	50,400	100,800	151,200	201,600
Annual capital charges	$C_{total}\ i\ (1+i)^n/[(1+n)^n - 1]$	294,782	400,507	490,102	569,867
Anual operating cost	Sum of the items above	1,564,784	2,612,709	3,635,609	4,643,259
Production cost ($/kg)	Annual operating cost divided by annual production output	2.76	2.75	2.74	2.72

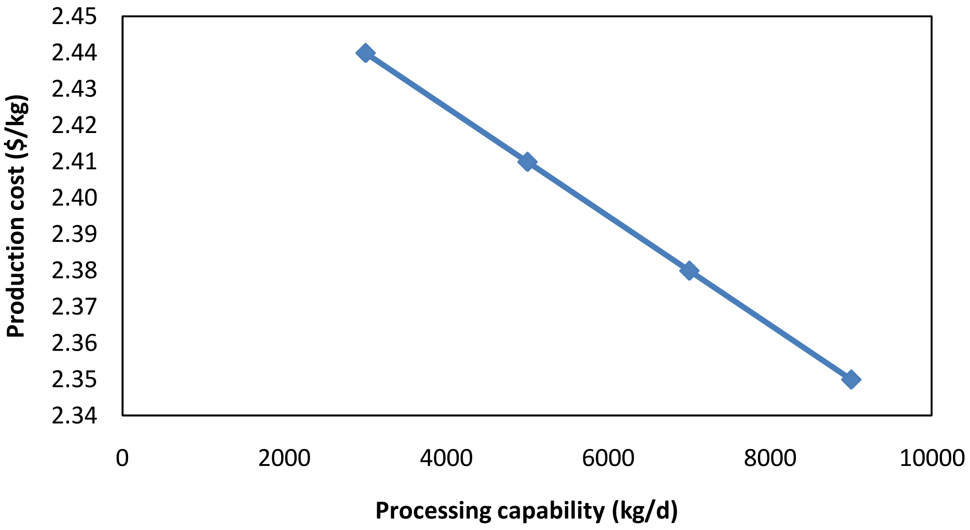

Figure 4.22. Production cost of activated carbon from fermentation residues at different production scales.

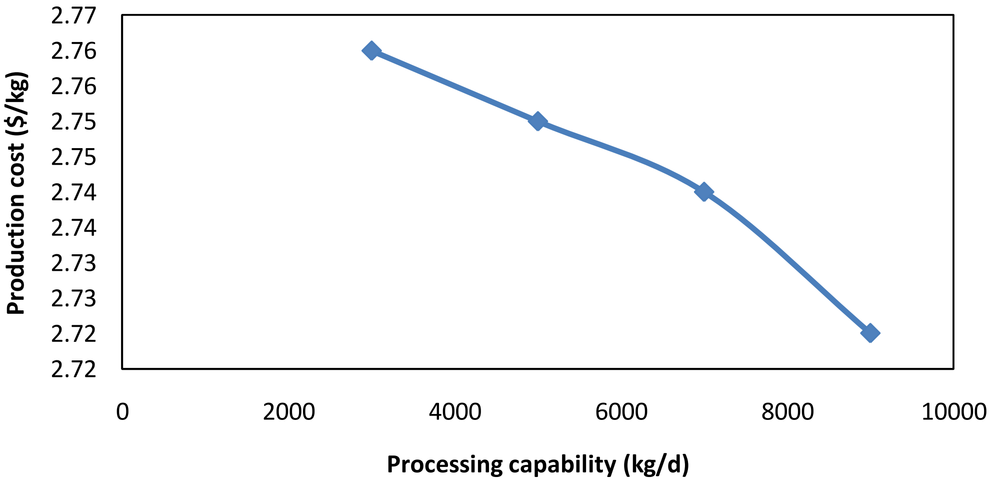

Figure 4.23. Production cost of activated carbon from pyrolysis residues at different production scales.

CHAPTER 5

CONCLUSION

1. Fermentation and pyrolysis residues are appropriate as precursors to prepare activated carbons due to their high carbon content and low ash content.
2. Fermentation residues have lower ash content than agricultural residues of the same origin because pretreatment, hydrolysis and fermentation processes wash some ash away.
3. Pyrolysis residues have a much higher carbon and ash contents than fermentation residues and agricultural residues of the same origin.
4. Rudimentary porosity has been developed in pyrolysis residues or bio-char during pyrolysis, which can promote the porosity development during the carbon-KOH activation reaction.
5. The increase of activation temperature, acid concentration and activation time decreased the yield of the activated carbon produced from fermentation residues.
6. The increase of activation temperature and time decreased the BET surface area and pore volume of activated carbon produced from fermentation residues while the acid concentration at 20% generated the higher BET surface area and pore volume than both acid concentrations of 10% and 30%.
7. BET surface area and pore volume of activated carbon produced from fermentation residues with H_3PO_4 activation are much lower than those of activated carbon produced from pyrolysis residues with KOH activation.

8. Activated carbon produced from pyrolysis residues have higher adsorption capacity than that produced from fermentation residues.
9. Optimized conditions for producing activated carbon from fermentation residues cannot be used to produce activated carbon from agricultural residues with the same quality.
10. Production cost of activated carbon from fermentation residues is lower than that of activated carbon from pyrolysis residues
11. The increase of production scale can reduce the production cost of activated carbon.

REFERENCES

[1] J. Sun, E. Hippo, H. Marsh, W. Brien, J. Crelling. Activated carbons produced from an Illinois basin coal. Carbon 1997; 35: 341–352.

[2] L. Hsu, H. Teng. Influence of different chemical reagents on the preparation of activated carbons from bituminous coal. Fuel Processing Technology 2000; 64: 155–166.

[3] H. Marsh, R. Menendez. Carbons from pyrolysis of pitches, coals, and their blends. Fuel Processing Technology 1988; 20: 269–296.

[4] S. Yorgun, N. Vural, H. Demiral. Preparation of high-surface area activated carbons from Paulownia wood by $ZnCl_2$ activation. Microporous and Mesoporous Materials 2009; 122: 189–194.

[5] V. Gómez-Serrano, E. M. Cuerda-Correa, M. Fernández-González, M. Alexandre-Franco, A. Macías-García. Preparation of activated carbons from chestnut wood by phosphoric acid-chemical activation. Study of microporosity and fractal dimension. Materials Letters 2005; 59: 846–853.

[6] E. Taer, M. Deraman, I. Talib, A. Umar, M. Oyama, R. Yunus. Physical, electrochemical and super capacitive properties of activated carbon pellets from pre-carbonized rubber wood sawdust by CO_2 activation. Current Applied Physics 2010; 10: 1071–1075.

[7] B. Kumar, K. Shivakamy, L. Miranda, M. Velan. Preparation of steam activated carbon from rubber wood sawdust (Hevea brasiliensis) and its adsorption kinetics. Journal of Hazardous Materials 2006; 136: 922–929.

[8] H. Demiral, G. Gündüzoğlu. Removal of nitrate from aqueous solutions by activated carbon prepared from sugar beet bagasse. Bioresource Technology 2010; 101:1675–1680.

[9] N. Amin. Removal of reactive dye from aqueous solutions by adsorption onto activated carbons prepared from sugarcane bagasse pith. Desalination 2008; 223:152–161.

[10] W. Li, K. Yang, J. Peng, L. Zhang, S. Guo, H. Xia. Effects of carbonization temperatures on characteristics of porosity in coconut shell chars and activated carbons derived from carbonized coconut shell chars. Industrial Crops and Products2008; 28: 190–198.

[11] K. Yang, J. Peng, C. Srinivasakannan, L. Zhang, H. Xia, X. Duan. Preparation of high surface area activated carbon from coconut shells using microwave heating. Bioresource Technology 2010; 101: 6163–6169.

[12] D. Prahas, Y. Kartika, N. Indraswati, S. Ismadji. Activated carbon from jackfruit peel waste by H_3PO_4 chemical activation: Pore structure and surface chemistry characterization. Chemical Engineering Journal 2008; 140: 32–42.

[13] B. Inbaraj, N. Sulochana. Carbonized jackfruit peel as an adsorbent for the removal of Cd(II) from aqueous solution. Bioresource Technology 2004; 94: 49–52.

[14] A. El-Sheikh, A. Newman, H. Al-Daffaee, S. Phull, N. Cresswell. Characterization of activated carbon prepared from a single cultivar of Jordanian Olive stones by chemical and physicochemical techniques. Journal of Analytical and Applied Pyrolysis 2004; 71:151–164.

[15] M. Martínez, M. Torres, C. Guzmán, D. Maestri. Preparation and characteristics of activated carbon from olive stones and walnut shells. Industrial Crops and Products 2006; 23: 23–28.

[16] A. Attia, B. Girgis, N. Fathy. Removal of methylene blue by carbons derived from peach stones by H_3PO_4 activation: Batch and column studies. Dyes and Pigments 2008; 76: 282–289.

[17] P. Vázquez, L. Pizzio, M. Blanco, C. Cáceres, H. Thomas, R. Arriagada, S.Bendezú, R. Cid, R. García. NiMo(W)-based hydrotreatment catalysts supported on peach stones activated carbon. Applied Catalysis A: General 1999; 184: 303–313.

[18] D. Kalderis, S. Bethanis, P. Paraskeva, E. Diamadopoulos. Production of activated carbon from bagasse and rice husk by a single-stage chemical activation method at low retention times. Bioresource Technology 2008; 99: 6809–6816.

[19] D. Kalderis, D. Koutoulakis, P. Paraskeva, E. Diamadopoulos, E. Otal, J. Valle, C. Fernández-Pereira. Adsorption of polluting substances on activated carbons prepared from rice husk and sugarcane bagasse. Chemical Engineering Journal 2008; 144: 42–50.

[20] K. Li, Z. Zheng, X. Huang, G. Zhao, J. Feng, J. Zhang. Equilibrium, kinetic and thermodynamic studies on the adsorption of 2-nitroaniline onto activated carbon prepared from cotton stalk fibre. Journal of Hazardous Materials 2009; 166: 213–220.

[21] H. Deng, L. Yang, G. Tao, J. Dai. Preparation and characterization of activated carbon from cotton stalk by microwave assisted chemical activation—Application in methylene blue adsorption from aqueous solution. Journal of Hazardous Materials 2009; 166:1514–1521.

[22] A. Lua, J. Guo. Activated carbon prepared from oil palm stone by one-step CO_2 activation for gaseous pollutant removal. Carbon 2000; 38: 1089–1097.

[23] T. Yang, A. Lua. Characteristics of activated carbons prepared from pistachio-nut shells by physical activation. Journal of Colloid and Interface Science 2003; 267: 408–417.

[24] V. Minkova, M. Razvigorova, M. Goranova, L. Ljutzkanov, G. Angelova. Effect of water vapor on the pyrolysis of solid fuels: effect of the yield and composition of liquid products . Fuel 1991; 70: 713–719.

[25] A. Marcilla, S. García-García, M. Asensio, J. Conesa. Influence of thermal treatment regime on the density and reactivity of activated carbons from almond shells. Carbon2000; 38: 429–440.

[26] C. Namasivayam, K. Kadirvelu. Activated carbons prepared from coir pith by physical and chemical activation methods. Bioresource Technology 1997; 62: 123–127.

[27] J. Maciá-Agulló, B. Moore, D. Cazorla-Amorós, A. Linares-Solano. Activation of coal tar pitch carbon fibres: Physical activation vs. chemical activation. Carbon 2004; 42: 1367–1370.

[28] A. Aworn, P. Thiravetyan, W. Nakbanpote. Preparation and characteristics of agricultural waste activated carbon by physical activation having micro- and and mesopores. Journal of Analytical and Applied Pyrolysis 2008; 82: 279–285.

[29] E. Arenas, F. Chejne. The effect of the activating agent and temperature on the porosity development of physically activated coal chars. Carbon 2004; 42: 2451–2455.

[30] P. Williams, A. Reed. Development of activated carbon pore structure via physical and chemical activation of biomass fibre waste. Biomass and Bioenergy 2006; 30: 144–152.

[31] E. Schröder, K. Thomauske, C. Weber, A. Hornung, V. Tumiatti. Experiments on the generation of activated carbon from biomass. Journal of Analytical and Applied Pyrolysis 2007; 79: 106–111.

[32] K. Okada, N. Yamamoto, Y. Kameshima, A. Yasumori. Porous properties of activated carbons from waste newspaper prepared by chemical and physical activation. Journal of Colloid and Interface Science 2003; 262: 179–193.

[33] T. Zhang, W. Walawender, L. Fan, M. Fan, D. Daugaard, R. Brown. Preparation of activated carbon from forest and agricultural residues through CO_2 activation. Chemical Engineering Journal 2004; 105: 53–59.

[34] N. Yalçın, V. Sevinç. Studies of the surface area and porosity of activated carbons prepared from rice husks. Carbon 2000; 38: 1943–1945.

[35] W. Daud, W. Ali, M. Sulaiman. The effects of carbonization temperature on pore development in palm-shell-based activated carbon. Carbon 2000; 38: 1925–1932.

[36] A. Ahmadpour, D. Do. The preparation of activated carbons from coal by chemical and physical activation. Carbon 1996; 34: 471–479.

[37] T. Budinova, E. Ekinci, F. Yardim, A. Grimm, E. Björnbom, V. Minkova, M. Goranova. Characterization and application of activated carbon produced by H_3PO_4 and water vapor activation. Fuel Processing Technology 2006; 87: 899–905.

[38] B. Girgis, A. Attia, N. Fathy. Modification in adsorption characteristics of activated carbon produced by H_3PO_4 under flowing gases. Colloids and Surfaces A: Physicochemical and Engineering Aspects 2007; 299: 79–87.

[39] S. Uçar, M. Erdem, T. Tay, S. Karagöz. Preparation and characterization of activated carbon produced from pomegranate seeds by $ZnCl_2$ activation. Applied Surface Science 2009; 255: 8890–8896.

[40] M. Olivares-Marín, C. Fernández-González, A. Macías-García, V. Gómez-Serrano. Preparation of activated carbon from cherry stones by chemical activation with $ZnCl_2$. Applied Surface Science 2006; 252: 5967–5971.

[41] Y. Sudaryanto, S. Hartono, W. Irawaty, H. Hindarso, S. Ismadji. High surface area activated carbon prepared from cassava peel by chemical activation. Bioresource Technology 2006; 97: 734–739.

[42] C. Hu, C. Wang, F. Wu, R. Tseng. Characterization of pistachio shell-derived carbons activated by a combination of KOH and CO_2 for electric double-layer capacitors. Electrochimica Acta 2007; 52: 2498–2505.

[43] R. Tseng, S. Tseng. Pore structure and adsorption performance of the KOH-activated carbons prepared from corncob. Journal of Colloid and Interface Science 2005; 287: 428–437.

[44] M. Jagtoyen, F. Derbyshire. Activated carbon from yellow poplar and white oak by H_3PO_4 activation. Carbon 1998; 36: 1085–1097.

[45] B. Girgis, E. Smith, M. Louis, A. El-Hendawy. Pilot production of activated carbon from cotton stalks using H_3PO_4. Journal of Analytical and Applied Pyrolysis2009; 86: 180–184.

[46] R. Yavuz, H. Akyildiz, N. Karatepe, E. Cetinkaya. Influence of preparation conditions on porous structures of olive stone activated by H_3PO_4. Fuel Processing Technology2010; 91: 80–87.

[47] T. Kawano, M. Kubota, M. Onyango, F. Watanabe, H. Matsuda. Preparation of activated carbon from petroleum coke by KOH chemical activation for adsorption heat pump. Applied Thermal Engineering 2008; 28: 865–871.

[48] G. Stavropoulos, A. Zabaniotou. Production and characterization of activated carbons from olive-seed waste residue. Microporous and Mesoporous Materials 2005; 82: 79–85.

[49] N. Khalili, M. Campbell, G. Sandi, J. Gola. Production of micro and mesoporous activated carbon from paper mill sludge: I. Effect of zinc chloride activation. Carbon 2000; 38: 1905–1915.

[50] M. Molina-Sabio, C. Almansa, F. Rodríguez-Reinoso. Phosphoric acid activated carbon discs for methane adsorption. Carbon 2003; 41: 2113–2119.

[51] H. Teng, S. Wang. Preparation of porous carbons from phenol-formaldehyde resins with chemical and physical activation. Carbon 2000; 38: 817–824.

[52] A. Marcilla, S. García-García, M. Asensio, J. Conesa. Influence of thermal treatment regime on the density and reactivity of activated carbons from almond shells. Carbon 2000; 38: 429–440.

[53] P. Malik. Use of activated carbons prepared from sawdust and rice-husk for adsorption of acid dyes: a case study of Acid Yellow 36. Dyes and Pigments 2003; 56: 239–249.

[54] G. Oh, C. Park. Preparation and characteristics of rice-straw-based porous carbons with high adsorption Capacity. Fuel 2002; 81: 327–336.

[55] T. Chuah, A. Jumasiah, I. Azni, S. Katayon, S. Choong. Rice husk as a potentially low-cost biosorbent for heavy metal and dye removal: an overview. Desalination 2005; 175: 305–316.

[56] S. Ricordel, S. Taha, I. Cisse, G. Dorange. Heavy metals removal by adsorption onto peanut husks carbon: characterization, kinetic study and modeling. Separation and Purification Technology 2001; 24: 389–401.

[57] A. Edrisa, B. Girgisb, H. Fadel. Recovery of volatile aroma components from aqueous waste streams using an activated carbon column. Food Chemistry 2003; 82: 195–202.

[58] A. Daifullah, B. Girgis, H. Gad. Utilization of agro-residues (rice husk) in small waste water treatment plans. Materials Letters 2003; 57: 1723–1731.

[59] A. El-Sheikh, A. Newman, H. Al-Daffaee, S. Phull, N. Cresswell. Characterization of activated carbon prepared from a single cultivar of Jordanian Olive stones by chemical and physicochemical techniques. Journal of Analytical and Applied Pyrolysis 2004; 71: 151–164.

[60] A. Dąbrowski, P. Podkościelny, Z. Hubicki, M. Barczak. Adsorption of phenolic compounds by activated carbon—a critical review. Chemosphere 2005; 58: 1049–1070.

[61] G. Dursun, H. Çiçek, A. Dursun. Adsorption of phenol from aqueous solution by using carbonized beet pulp. Journal of Hazardous Materials 2005; 125: 175–182.

[62] M. Yates, J. Blanco, P. Avila, M. Martin. Honeycomb monoliths of activated carbons for effluent gas Purification. Microporous and Mesoporous Materials 2000; 37: 201–208.

[63] S. Vitolo, M. Seggiani. Mercury removal from geothermal exhaust gas by sulfur-impregnated and virgin activated carbons. Geothermics 2002; 31: 431–442.

[64] T. Yang, A. Lua. Characteristics of activated carbons prepared from pistachio-nut shells by physical activation. Journal of Colloid and Interface Science 2003; 267: 408–417.

[65] S. Biloé, V. Goetz, A. Guillot. Optimal design of activated carbon for an adsorbed natural gas storage system. Carbon 2002; 40: 1295–1308.

[66] P. Georgiev, D. Ross, P. Albers, A. Ramirez-Cuesta. The rotational and translational dynamics of molecular hydrogen physisorbed in activated carbon: A direct probe of microporosity and hydrogen storage performance. Carbon 2006; 44: 2724–2738.

[67] K. Inomata, K. Kanazawa, Y. Urabe, H. Hosono, T. Araki. Natural gas storage in activated carbon pellets without a binder. Carbon 2002; 40: 87-93.

[68] M. Jordá-Beneyto, D. Lozano-Castelló, F. Suárez-García, D. Cazorla-Amorós, Á. Linares-Solano. Advanced activated carbon monoliths and activated carbons for hydrogen storage. Microporous and Mesoporous Materials 2008; 112: 235–242.

[69] X. Zheng, S. Zhang, J. Xu, K. Wei. Effect of thermal and oxidative treatments of activated carbon on its surface structure and suitability as a support for barium promoted ruthenium in ammonia synthesis catalysts. Carbon 2002; 40: 2597–2603.

[70] M. Gurrath, T. Kuretzky, H. Boehm, L. Okhlopkova, A. Lisitsyn, V. Likholobov. Palladium catalysts on activated carbon supports. Influence of reduction temperature, origin of the support and pretreatments of the carbon surface. Carbon 2000; 38: 1241–1255.

[71] M. Kang, Y. Bae, C. Lee. Effect of heat treatment of activated carbon supports on the loading and activity of Pt catalyst. Carbon 2005; 43: 1512–1516.

[72] C. Ao, S. Lee. Indoor air purification by photo catalyst TiO_2 immobilized on an activated carbon filter installed in an air cleaner. Chemical Engineering Science 2005; 60: 103–109.

[73] A. Bagreev, F. Adib, T. Bandosz. PH of activated carbon surface as an indication of its suitability for H_2S removal from moist air streams. Carbon 2001; 39: 1897–1905.

[74] K. Adani, R. Barley, R. Pascoe. Silver recovery from synthetic photographic and medical X-ray process effluents using activated carbon. Minerals Engineering 2005; 18: 1269–1276.

[75] L. Barnes, G. Phillips, J. Davies, A. Lloyd, E. Cheek, S. Tennison, A. Rawlinson, O. Kozynchenko, S. Mikhalovsky. The cytotoxity of highly porous medical carbon adsorbents. Carbon 2009; 47: 1887-1895.

[76] A. Smolka, K. Schmidt. Gas/partical partitioning before and after flue gas purification by an activated-carbon-filter. Chemosphere 1997; 34: 1075–1082.

[77] F. López, F. Medina, M. Prodanov, C. Güell. Oxidation of activated carbon: application to vinegar decolorization. Colloid and Interface Science 2003; 257: 173–178.

[78] C. Ng, W. Marshall, R. Rao, R. Bansode, J. Losso. Activated carbon from pecan shell: process description and economic analysis. Industrial Crops and Products 2003; 17: 209– 217.

[79] G. Stavropoulos, A. Zabaniotou. Minimizing activated carbons production cost. Fuel Processing Technology 2009; 90: 952-957.

[80] K. Choy, J. Barford, G. McKay. Production of activated carbon from bamboo scaffolding waste – process design, eva;uation and sensitivity analysis. Chemical Engineering Journal 2005; 109: Pages 147-165.

[81] P. Bayer, E. Heuer, U. Karl, M. Finkel. Economical and ecological comparison of granular activated carbon (GAC) adsorber refill strategies. Water Research 2005; 39: 1719-1728.

[82] C. Toles, W. Marshall, M. Johns, L. Wartelle, A. McAloon. Acid activated carbons from almond shells: physical, chemical and adsorptive properties and estimated cost of production. Bioresource Technology 2000; 71: 87-92.

[83] C. Toles, W. Marshall, L. Wartelle, A. McAloon. Steam or carbon dioxide activated carbon from almond shells: physical, chemical and adsorptive properties and estimated cost of production Bioresource Technology 2000; 75: 197-203.

[84] S. Zuo, J. Yang, J. Liu, X. Cai. Significance of the carbonization of volatile pyrolytic productis on the properties of activated carbons from phosphoric acid activation of lignocellulosic material. Fuel Processing Technology 2009; 90: 994-1001.

[85] Q. Liu, T. Zheng, P. Wang, L. Guo. Preparation and characterization of activated carbon from bamboo by micro-wave induced phosphoric acid activation. Industrial Crops and Products 2010; 31: 233-238.

[86] T. Vernersson, P. Bonelli, E. Cerrella, A. Cukierman. Arundo donax cane as a precursor for activated carbon preparation by phosphoric acid activation. Bioresource Technology 2002; 83: 95-104.